Radiative corrections to aid the direct detection of the Higgsino-like neutralino dark matter: Spin-independent interactions

Subhadip Bisal,[1,2,*] Arindam Chatterjee,[3,†] Debottam Das,[1,2,‡] and Syed Adil Pasha[3,§]

[1]*Institute of Physics, Sachivalaya Marg, Bhubaneswar 751 005, India*
[2]*Homi Bhabha National Institute, Training School Complex, Anushakti Nagar, Mumbai 400 094, India*
[3]*Shiv Nadar IoE Deemed to be University, Gautam Buddha Nagar, Uttar Pradesh 201314, India*

(Received 8 March 2024; accepted 29 June 2024; published 30 July 2024)

The lightest neutralino ($\tilde{\chi}_1^0$) is a good dark matter (DM) candidate in the R-parity conserving minimal supersymmetric Standard Model. In this work, we consider the light Higgsino-like neutralino as the lightest stable particle, thanks to a rather small Higgsino mass parameter μ. We then estimate the prominent radiative corrections to the neutralino-neutralino-Higgs boson vertices. We show that for Higgsino-like $\tilde{\chi}_1^0$, these corrections can significantly influence the spin-independent direct detection cross section, even contributing close to 100% in certain regions of the parameter space. These corrections, therefore, play an important role in deducing constraints on the mass of the Higgsino-like lightest neutralino DM, and thus the μ parameter.

DOI: 10.1103/PhysRevD.110.023043

I. INTRODUCTION

A prime motivation for supersymmetric extensions of the standard model of particle physics (SM) have been to address the "naturalness" concerns. While there are several studies in literature to quantify "naturalness" in a supersymmetric framework, the measure of naturalness is often debated [1–7]. In the minimal supersymmetric extension of the standard model (MSSM), a small value of the Higgsino mass parameter μ [1,2,4,5] and possibly rather light stop squarks and gluinos ($\lesssim$2–3 TeV) [6–10] remain desirable in "natural" scenarios at the electroweak (EW) scale.

At the Large Hadron Collider (LHC), the discovery of the Higgs boson has established Standard Model (SM) physics. However, in spite of strong motivation for physics beyond the standard model, no hints for the same have been observed so far. The constraints on the supersymmetric spectrum [11–17], while generally dependent on the nature of the low-lying states, have been raising concerns about the naturalness requirements [6–10]. In this regard, within the minimal supersymmetric standard model (MSSM) paradigm, the constraint on the μ parameter is of particular interest. This has been widely studied in literature in the light of LHC.[1] In the minimal construct, a small Higgsino mass parameter μ [of $\mathcal{O}(100)$ GeV] is of relevance.[2] Assuming that the gaugino mass parameters M_1 and M_2 are in the ballpark of multi-TeV, such a scenario leads to a compressed Higgsino spectrum. In the R-parity conserving scenario, where the lightest supersymmetric particle (LSP) is stable. This leads to the Higgsino-like lightest neutralino being a dark matter (DM) candidate. Such a scenario attracts rather weak constraints from the electroweakino searches at the LHC, as the decay of the next two heavier (Higgsino-like) states lead to soft SM particles in the final states at the collider.

Several studies have considered the prospects and constraints on the lightest neutralino in the light of collider and DM searches. Also, the implications of a compressed Higgsino-like spectrum at the LHC have been studied widely [23–34]. While the neutralino and chargino pair production cross sections are sizable, especially for small μ, the soft decay products in the compressed spectrum ensure that the constraints are rather weak. With Higgsino-like neutralinos as DM candidates, a complimentary set of constraints on the μ parameter [33,35,36] also follow from the direct [37–40] and indirect [41–43] searches for DM.

*Contact author: subhadip.b@iopb.res.in
†Contact author: arindam.chatterjee@snu.edu.in
‡Contact author: debottam@iopb.res.in
§Contact author: sp855@snu.edu.in

[1]Within the high-scale supersymmetric models, a moderate value of the μ parameter may be realized in the focus point region [3,18–22].

[2]Note that, the fine-tuning measure, estimated following the electroweak naturalness criteria, is stated to be about $\mathcal{O}(10$–$100)$ assuming the masses of the third-generation squarks and gluons in the ballpark of several TeV [6].

In the present work, we revisit the implications of the spin-independent direct detection constraints on the Higgsino-like ($\tilde{\chi}_1^0$). As the coupling of CP-even neutral Higgs bosons with a pair of $\tilde{\chi}_1^0$ is vanishingly small at the tree level, the contribution to the spin-independent neutralino-nucleus interaction process is suppressed.[3] Consequently, the radiative contributions to the scattering process need to be considered in order to accurately estimate the relevant cross sections. While such a scenario has been previously considered in the literature, in the context of pure Higgsinos, the importance of radiative corrections to the direct detection process has received some attention [47–50].[4]

We improve the estimation of the radiative corrections to the spin-independent direct detection cross section, by incorporating the contributions from the gauge bosons, the Higgs bosons, the respective superpartners and the third-generation (s)quarks to the relevant vertices involving neutralino and Higgs bosons. Further, we renormalize the chargino-neutralino sector using the use the on shell renormalization scheme and estimate the relevant vertex counterterms, thus paving the way towards a full one-loop treatment to the neutralino-Higgs boson vertices.

In order to satisfy the thermal relic abundance of $\Omega_{\rm DM}h^2 \simeq 0.12$, as required by cosmological considerations [59,60], the Higgsino-like neutralino LSP must be around 1 TeV and can be lowered further in the presence of coannihilation [33]. Below this mass scale, it is generally under abundant. However, there are viable nonthermal production scenarios, where adequate production of such DM may be possible in the early Universe [61,62]. Further, the presence of additional DM components, e.g., axions, may contribute to the DM abundance [44,63,64]. In this work, we will not concern ourselves with satisfying the thermal relic abundance in the early Universe. We will only focus on the impact of certain radiative corrections on such a DM candidate in the light of direct DM searches. Note that if the LSP constitutes only a fraction of the required DM relic abundance (and, therefore, the local DM density), the constraint on the DM-nucleon scattering cross section from direct searches will be relaxed in the same proportion.

This article is organized as follows. In Sec. II, the chargino-neutralino spectrum of interest has been described, and the tree-level interactions between $\tilde{\chi}_1^0$ and the CP-even Higgs bosons are described. Following this, in Sec. III, the generalities of (spin-independent direct detection of DM and the implications in the context of a Higgsino-like DM candidate have been discussed. Subsequently, in Sec. IV, we present the important electroweak radiative corrections to the vertices involving neutralino and the Higgs bosons and study its impact on the spin-independent DM-nucleon cross sections. We also reflect on the parameter region where such corrections are significant and comment on the implications on the viable region for the Higgsino mass parameter μ. Finally, in Sec. V, we summarize the results and conclude.

[3]We note in passing that for a mixed LSP, significant parts of the MSSM parameter space have been ruled out by direct directions constraints unless one hits the "blind spot" [44,45]; a similar situation arises if one tunes the Yukawa parameters leading to cancellation among different contributing processes [46].

[4]Certain classes of radiative corrections to the direct detection process and the relic abundance in the context of neutralino DM have been studied in Refs. [51–58].

II. THE FRAMEWORK

In this section, we briefly discuss the chargino-neutralino sector in the MSSM; in particular, we focus on the parameter region with rather small Higgsino mass parameter μ and light Higgsino-like states.

A. The spectrum: Compressed Higgsinos

In the gauge eigenbasis expressed in terms of the Weyl spinors (the charged wino ($\tilde{W}^{\pm}$), and charged Higgsinos ($\tilde{h}_i^{\pm}$), for $i \in \{1,2\}$) with $\psi^+ = (\tilde{W}^+, \tilde{h}_2^+)^T$ and $\psi^- = (\tilde{W}^-, \tilde{h}_1^-)^T$, the tree-level mass term for the charginos is given by [65]

$$-\mathcal{L}^{\rm c}_{\rm mass} = \psi^{-T} M^{c} \psi^{+} + \text{H.c.} \tag{1}$$

The mass matrix $M^{\rm c}$ can be expressed as

$$M^{\rm c} = \begin{pmatrix} M_2 & \sqrt{2}M_W \sin\beta \\ \sqrt{2}M_W \cos\beta & \mu \end{pmatrix}. \tag{2}$$

Here M_2 and μ stand for the supersymmetry breaking $SU(2)$ wino mass parameter and the supersymmetric Higgsino mass parameter, respectively. M_W is the mass of the W boson, and $\tan\beta$ is the ratio of the vacuum expectation values (VEVs) of the up-type and the down-type CP-even neutral Higgs bosons. The matrix $M^{\rm c}$ can be diagonalized with a biunitary transformation using the unitary matrices U and V to obtain,

$$M^{\rm c}_D = U^* M^{\rm c} V^{-1} = \text{Diagonal}(m_{\tilde{\chi}_1^+} m_{\tilde{\chi}_2^+}). \tag{3}$$

The eigenstates are ordered such that $m_{\tilde{\chi}_1^+} \leq m_{\tilde{\chi}_2^+}$. The left- and right-handed components of these mass eigenstates, the charginos ($\tilde{\chi}_i^+$ with $i \in \{1,2\}$), are

$$P_L \tilde{\chi}_i^+ = V_{ij} \psi_j^+, \qquad P_R \tilde{\chi}_i^+ = U_{ij}^* \overline{\psi_j^-}, \tag{4}$$

where P_L and P_R are the usual projectors, $\overline{\psi_j^-} = \psi_j^{-\dagger}$, and summation over j is implied.

For the neutralino states, in the gauge eigenbasis [consisting of the bino ($\tilde{B}^0$), neutral wino ($\tilde{W}^3$), and down-type and up-type neutral Higgsinos ($\tilde{h}_1^0$ and $\tilde{h}_2^0$ respectively)],

$\psi^0 = (\tilde{B}^0, \tilde{W}^3, \tilde{h}_1^0, \tilde{h}_2^0)^T$, the mass term takes the following form [65]:

$$-\mathcal{L}_{\text{mass}}^{\text{n}} = \frac{1}{2}\psi^{0T} M^n \psi^0 + \text{H.c.} \tag{5}$$

The neutralino mass matrix M^{n} is given by

$$M^{\text{n}} = \begin{pmatrix} M_1 & 0 & -M_Z s_W c_\beta & M_Z s_W s_\beta \\ 0 & M_2 & M_Z c_W c_\beta & -M_Z c_W s_\beta \\ -M_Z s_W c_\beta & M_Z c_W c_\beta & 0 & -\mu \\ M_Z s_W s_\beta & -M_Z c_W s_\beta & -\mu & 0 \end{pmatrix}. \tag{6}$$

In the above equation s_W, s_β, c_W, and c_β stand for $\sin\theta_W, \sin\beta, \cos\theta_W$, and $\cos\beta$, respectively while θ_W is the weak mixing angle. M_Z is the mass of the Z boson, and M_1 is the supersymmetry breaking $U(1)_Y$ gaugino (bino) mass parameter. M^{n} can be diagonalized by a unitary matrix N to obtain the masses of the neutralinos as follows:

$$M_D^{\text{n}} = N^* M^{\text{n}} N^{-1} = \text{Diagonal}(m_{\tilde{\chi}_1^0} m_{\tilde{\chi}_2^0} m_{\tilde{\chi}_3^0} m_{\tilde{\chi}_4^0}). \tag{7}$$

The eigenstates ($\tilde{\chi}_i^0$) are ordered according to the respective mass eigenvalues as follows,[5] $m_{\tilde{\chi}_1^0} \leq m_{\tilde{\chi}_2^0} \leq m_{\tilde{\chi}_3^0} \leq m_{\tilde{\chi}_4^0}$. These eigenstates satisfy $\tilde{\chi}_i^{0c} = \tilde{\chi}_i^0$, where the superscript c stands for charge conjugation. The left-handed components of these mass eigenstates, the Majorana neutralinos, $\tilde{\chi}_i^0$ ($i \in \{1,2,3,4\}$), may be obtained as

$$P_L \tilde{\chi}_i^0 = N_{ij} \psi_j^0, \tag{8}$$

where summation over j is again implied.

The analytical expressions corresponding to the chargino and the neutralino mass eigenvalues have been obtained in the literature [66,67]. However, a numerical estimation of the eigenvalues is straightforward and convenient, especially in the case of the neutralinos.

In the region of interest in this article, the Higgsino mass parameter is rather small in comparison with the gaugino and the wino mass parameters, i.e., $|\mu| \ll |M_1|, M_2$; the masses of the light Higgsino-like particles may be approximately given by [47,68][6]

$$\begin{aligned} m_{\tilde{\chi}_1^\pm} &= |\mu|\left(1 - \frac{M_W^2 \sin 2\beta}{\mu M_2}\right) + \mathcal{O}(M_2^{-2}) + \text{rad corr} \\ m_{\tilde{\chi}_{a,s}^0} &= \pm\mu - \frac{M_Z^2}{2}(1 \pm \sin 2\beta)\left(\frac{\sin\theta_W^2}{M_1} + \frac{\cos\theta_W^2}{M_2}\right) \\ &\quad + \text{rad corr}. \end{aligned} \tag{9}$$

[5]Note that some of the eigenvalues may be negative depending on the input parameters. In such cases, the chiral rotation of the corresponding mass eigenstate may be performed to change the sign of the eigenvalue.

[6]An exact analytical result may be found in Refs. [69,70].

In the above expression, subscripts $a(s)$ refer to antisymmetric (symmetric) combinations of up-type ($\tilde{h}_2^0$) and down-type ($\tilde{h}_1^0$) Higgsinos constituting the respective mass eigenstates. Here, the symmetric and antisymmetric states refer to the Higgsino-like states with compositions without and with a relative sign between N_{i3} and N_{i4}, respectively. It has been pointed out in the literature that, due to the mixing effects, the mass differences $\Delta m_1 = m_{\tilde{\chi}_1^\pm} - m_{\tilde{\chi}_1^0}$ may become very small in certain regions of the parameter space [27,29,71,72]. In the present context, we will consider the mass differences $\Delta m_1, \Delta m_2 \gg \mathcal{O}(1\ \text{MeV})$. Thus, as we will discuss in the next section, in the direct detection experiments, only the elastic scattering of $\tilde{\chi}_1^0$ with the nucleon will be relevant.

B. Neutralino-Higgs boson(s) interaction: Tree-level and at one loop

As we will elaborate on in Sec. III, for the spin-independent direct detection of $\tilde{\chi}_1^0$, the relevant vertices involve the lightest neutralino and the CP-even Higgs bosons. The gauge symmetry of the MSSM, particularly the electroweak gauge group, prohibits any superpotential term with two Higgsino states and a Higgs boson in the gauge eigenbasis. Therefore, the tree-level interaction term, in the gauge eigenbasis, involves one Higgsino, one gaugino, and a Higgs boson. Consequently, in the mass eigenbasis, the tree-level vertex takes the following form [65]:

$$\begin{aligned} \mathcal{L} \supset &-\frac{1}{2} h_1 \bar{\tilde{\chi}}_1^0 (\mathcal{C}_1^R P_R + \mathcal{C}_1^L P_L) \tilde{\chi}_1^0 \\ &-\frac{1}{2} h_2 \bar{\tilde{\chi}}_1^0 (\mathcal{C}_2^R P_R + \mathcal{C}_2^L P_L) \tilde{\chi}_1^0, \end{aligned} \tag{10}$$

where $\mathcal{C}_i^L = \mathcal{C}_i^{R*}$ for $i \in \{1,2\}$, and

$$\mathcal{C}_1^R = (S_1 \sin\alpha + S_2 \cos\alpha), \tag{11}$$

$$\mathcal{C}_2^R = (S_2 \sin\alpha - S_1 \cos\alpha), \tag{12}$$

$$S_1 = g_2 N_{13}(N_{12} - \tan\theta_W N_{11}), \tag{13}$$

$$S_2 = g_2 N_{14}(N_{12} - \tan\theta_W N_{11}). \tag{14}$$

In the above expressions, h_1 and h_2 denote the 125 GeV Higgs boson and the heavy Higgs boson mass eigenstates, respectively, g_2 denotes the $SU(2)$ gauge coupling, and α denotes the mixing angle in the CP-even Higgs sector. Note that in the above equations, N_{11} and N_{12} denote the bino and wino composition of the lightest neutralino mass eigenstate, while N_{13}^2 and N_{14}^2 denote the respective down-type and up-type Higgsino fractions in the $\tilde{\chi}_1^0$, respectively. For Higgsino-like $\tilde{\chi}_1^0$, the gaugino fraction is very small compared to the Higgsino fraction, i.e., $|N_{13}|^2 + |N_{14}|^2 \gg |N_{11}|^2 + |N_{12}|^2$. Thus, the tree-level vertex involving the

CP-even Higgs bosons is suppressed by a rather small gaugino component of the mixing matrix (i.e., N_{11} and N_{12}). As pointed out, the radiative corrections to these vertices play an important role in the spin-independent direct detection process; this will be illustrated in Sec. IV.

To treat the interaction Lagrangian at one-loop level, the counterterm Lagrangian $\mathcal{L}_{\rm CT}$ should be added to the tree-level Lagrangian $\mathcal{L}_{\rm tree}$. The Lagrangian, thus takes the following form:

$$\mathcal{L} = \mathcal{L}_{\rm Born} + \mathcal{L}_{\rm CT}, \tag{15}$$

where $\mathcal{L}_{\rm Born}$ is written using the renormalized fields, and $\mathcal{L}_{\rm CT}$ involves the contributions from the relevant counterterms. The "bare" and the renormalized neutralino mass eigenstates are related as follows:

$$\tilde{\chi}_i^{0\,\rm bare} = \left(\delta_{ij} + \frac{1}{2}\delta Z_{ij} P_L + \frac{1}{2}\delta Z_{ij}^* P_R\right)\tilde{\chi}_j^{0\,\rm renormalized}, \tag{16}$$

where the index j has been summed over $j \in \{1,2,3,4\}$. The wave function renormalization counterterms δZ_{ij} are determined using the on shell renormalization schemes [73], a comparison among different variants can be found in Ref. [74]. Similarly, for the CP-even neutral Higgs bosons the bare and the renormalized mass eigenstates are related as follows:

$$h_i^{\rm bare} = \left(\delta_{ij} + \frac{1}{2}\delta Z_{ij}^{\rm H}\right) h_j^{\rm renormalized}, \tag{17}$$

where the index j has been summed over $j \in \{1,2\}$. The on shell renormalization prescription is used to determine the wave function renormalization counterterms δZ_{ij}^H. With the above relations, the counterterm Lagrangian $\mathcal{L}_{\rm CT}$ relevant for the present discussion can be obtained as follows:

$$\begin{aligned} -\mathcal{L}_{\rm CT} \supset\ & \frac{1}{2} h_1 \bar{\tilde{\chi}}_1^0 (\delta \mathcal{C}_1^R P_R + \delta \mathcal{C}_1^L P_L)\tilde{\chi}_1^0 \\ & + \frac{1}{2} h_2 \bar{\tilde{\chi}}_1^0 (\delta \mathcal{C}_2^R P_R + \delta \mathcal{C}_2^L P_L)\tilde{\chi}_1^0, \end{aligned}$$

where the renormalized fields are used in the counterterm Lagrangian; we have dropped the respective superscript. At the one-loop level, the neutralinos, charginos, gauge bosons, and the Higgs bosons contribute to the $\tilde{\chi}_1^0, \tilde{\chi}_1^0, h_i$ vertices. Further, there can be sizable contributions from the third-generation (s)quarks, thanks to the sizable Yukawa couplings, as will be discussed in Sec. IV. Note that for all our benchmark scenarios, as described in Sec. IV, the lightest eigenvalue of the neutralino mass matrix $M^{\rm n}$ is positive. Consequently, for the benchmarks presented in Sec. IV (Tables I and II), $\mathcal{C}_i^L = \mathcal{C}_i^R$ and $\delta\mathcal{C}_i^L = \delta\mathcal{C}_i^R$ for $i \in \{1,2\}$.

C. Constraints on the parameter space

A small $\mu \ll |M_1|, M_2$, as discussed above, leads to a compressed spectrum with three closely spaced states $\tilde{\chi}_1^0, \tilde{\chi}_2^0, \tilde{\chi}_1^\pm$. The LHC sets stringent limits on chargino and neutralino masses, from pair productions of charginos and neutralinos and the subsequent decay of those to $\tilde{\chi}_1^0$ and SM particles. These limits are sensitive to the mass difference of the heavier chargino and neutralino states and the LSP ($\tilde{\chi}_1^0$). As for small mass splittings, the relevant bounds on the compressed spectrum can be found in Refs. [15,75–77]. For 300 (600) GeV Higgsino-like neutralinos, $\Delta m_1 \lesssim 0.3(0.2)$ GeV is disfavored [77], and the constraints weaken for heavier mass. Searches targeting mass splittings around the electroweak scale may be found in Refs. [11–17], where decays of the heavier neutralinos into on shell gauge bosons or Higgs bosons and the LSP, as well as their three-body decays have been considered. However, as $|M_1|, M_2 \gg |\mu|$ in our context, these constraints are not very relevant to the present discussion. We have considered the following constraints on the spectrum for our benchmark scenarios presented in Sec. IV:

(i) We have constrained the lightest CP-even Higgs mass m_h within the range $122 \le m_h(\text{GeV}) \le 128$ [78–80]. Note that the experimental uncertainty is about 0.25 GeV and the uncertainty in the theoretical estimation of the Higgs mass is about ± 3 GeV, see e.g., [81] and references therein.

(ii) The squarks and the sleptons masses have been assumed to be above 1.5 TeV, and the gluino mass is kept above 2.2 TeV, respecting the constraints from the LHC.

(iii) In our scenario, with $|\mu| \ll |M_1|, M_2$, the low-lying Higgsino-like states form a compressed spectrum. The μ parameter has been chosen such that LHC constraints on the compressed spectra are respected [15,75,76]. We have also used `SModelS` (version-2.3.0) [82–90] to check our benchmark scenarios.

(iv) However, we have relaxed the constraints on the relic density of DM (i.e., $\Omega_{\rm DM} \simeq 0.12$). As $\tilde{\chi}_1^0$–may not constitute all of the DM, constraint from indirect searches on the Higgsino-like DM [36,41,42] has also been relaxed.

III. DIRECT DETECTION OF DARK MATTER: IMPLICATIONS FOR A HIGGSINO-LIKE LSP

A. Generalities of direct detection

In this section, we describe the generalities of spin-independent direct detection and sketch the implications for the Higgsino-like $\tilde{\chi}_1^0$–nucleon scattering. In the context of direct detection, the differential event rate per unit time at a detector, as a function of the nuclear recoil energy E_R, is given by

$$\frac{dR}{dE_R} = n_T \frac{\rho_{\tilde{\chi}_1^0}}{m_{\tilde{\chi}_1^0}} \int_{v_{\min}}^{v_{\rm esc}} d^3v f_E(\vec{v}) v \frac{d\sigma(v, E_R)}{dE_R}. \quad (18)$$

In the above equation, $\rho_{\tilde{\chi}_1^0}$ is the local density ($\simeq$0.3 GeV cm^{-3}), n_T is the number of target nuclei in the detector and $\sigma(v, E_R)$ denotes the scattering cross section with the nucleus. Further, $f_E(\vec{v})$ denotes the velocity distribution in the Earth's rest frame and $f_E(\vec{v}) = f(\vec{v} + \vec{v}_E)$, where f is the distribution function in the galactic rest frame and $\vec{v}_E$ is the velocity of Earth with respect to the galactic rest frame and $v_{\rm esc}$ is the escape velocity of our galaxy. Further, $v_{\min}^2 = \frac{m_T E_R}{2M_r^2}$ is the minimum speed of the DM particle required to impart a recoil energy E_R, where m_T is the mass of the target nucleus, and M_r is the reduced mass of the DM-nucleus system. The cross section with a nucleus (atomic number A and charge Z) is given by

$$\frac{d\sigma}{dE_R}(v, E_R) = \frac{m_T}{2M_r^2 v^2} \sigma_0 F^2(q^2), \quad (19)$$

where m_T is the mass of the target nucleus, $q^2 = 2m_T E_R$ is the square of the momentum transfer, and F stands for the form factor, which will be taken as the Woods-Saxon form factor [91]. Further, σ is the (spin-independent) DM-nucleus scattering cross section. In the present context only spin-independent cross section is relevant, which, at zero momentum transfer is given by σ_0.

B. Dark matter-nucleon spin-independent elastic scattering

In the following, we briefly discuss the relevant parton level effective Lagrangian leading to the spin-independent interaction [92],

$$\mathcal{L}_{\rm eff} \supset \lambda_q \bar{\tilde{\chi}}_1^0 \tilde{\chi}_1^0 \bar{q} q + g_q \bar{\tilde{\chi}}_1^0 \gamma^\mu \partial^\nu \tilde{\chi}_1^0 (\bar{q}\gamma_\mu \partial_\nu q - \partial_\mu \bar{q} \gamma_\nu q) + \mathcal{L}_{\rm eff}^g. \quad (20)$$

In the above equation, the first term in the right-hand side receives contributions largely from the scattering processes mediated by the Higgs bosons. In particular, in the limit of no mixing in the squark sector, the contribution from the squark sector to this operator vanishes [92,93]. The next term captures the effect of squark-mediated s-channel scattering processes. Further, $\mathcal{L}_{\rm eff}^g$ denotes the relevant effective interactions with gluons which contribute to the spin-independent neutralino nucleon scattering process [92,93].

We now focus on the implications for a Higgsino-like $\tilde{\chi}_1^0$, as we consider in the present context. For such states, the Higgsino fraction is much greater than the gaugino fraction (i.e., $|N_{13}|, |N_{14}| \gg |N_{11}|, |N_{12}|$). Therefore, the tree-level coupling involving two neutralinos and the Higgs bosons [see Eq. (14)] are small, as these are suppressed by a factor of the gaugino component of the Higgsino-like neutralino state. Note that, in the present context we consider $|M_1|, M_2 \lesssim 5$ TeV and the Higgsino mass parameter $|\mu| \lesssim 1$ TeV. Consequently, the gaugino fraction in the lightest neutralino is typically $\mathcal{O}(10^{-2})$. Thus, the tree-level Higgs boson exchange contributions, while small, can be significant and generally non-negligible. The tree-level contributions from the (s–channel) squark-mediated processes are suppressed by an additional factor of a rather small gaugino fraction in $\tilde{\chi}_1^0$ and/or an additional factor of Yukawa coupling for the first two generation of (s)quarks as compared to the tree-level Higgs boson exchange processes. Further, we have considered the first two generations of squarks to be very heavy ($\gg \mathcal{O}(2)$) TeV for all our benchmark scenarios, as will be described in Sec. IV. Therefore, contributions from the respective squark-mediated processes (and their contributions to the neutralino-gluon effective operators) remain subdominant in the present context. In the following, we first describe the Higgs exchange contribution, as the focus of the present study is on the radiative corrections to the neutralino-Higgs boson vertices.

The effective parton-level interactions, as mentioned in (20) leads to the following effective interaction Lagrangian with the nucleon $N \in \{n, p\}$, where n and p stand for neutron and proton, respectively,

$$\mathcal{L}_N^{\rm eff} \supset f_N \bar{\tilde{\chi}}_1^0 \tilde{\chi}_1^0 \bar{\psi}_N \psi_N, \quad (21)$$

where f_N denotes the effective coupling and ψ_N denotes the field describing the nucleon N. The important contributions from the two CP-even neutral Higgs boson mediated processes in the spin-independent cross section $\sigma_{\rm SI}$ comes from its contribution to the coefficient λ_q. The contribution from the two CP-even neutral Higgs bosons λ_q^H is given by

$$\lambda_q^H = \sum_{i=1}^{2} \frac{C_i C_{iq}}{m_{h_i}^2}. \quad (22)$$

In this expression, $C_i = \mathcal{C}_i^L$ as mentioned in (14) and C_{iq} denotes the coupling of the same Higgs boson and quark(q) [65]. The respective contribution to the spin-independent elastic scattering cross section may be expressed in terms of their contribution to the effective interaction strength f_N [92,94,95],

$$f_N^{(H)} = m_N \left(\sum_q^{u,d,s} f_{T_q}^N \frac{\lambda_q^H}{m_q} + \frac{2}{27} \sum_q^{c,b,t} f_{T_G}^N \frac{\lambda_q^H}{m_q} + \frac{8\pi}{9\alpha_S} f_{T_G}^N m_N T_{\tilde{q}} \right); \quad N \in \{p, n\}, \quad (23)$$

where [92,96],

$$f_{T_q}^N = \frac{1}{m_N} \langle N | m_q \bar{q} q | N \rangle, \qquad f_{T_G}^N = 1 - \sum_q^{u,d,s} f_{T_q}^N,$$

$$T_{\tilde{q}} = \frac{\alpha_S}{4\pi} \frac{1}{24} \sum_{i=1}^{2} \frac{C_i}{m_{h_i}^2} \sum_{\tilde{q}_j} \frac{C_{\tilde{q}_j}^i}{m_{\tilde{q}_j}^2}. \quad (24)$$

In the above equation, $f^N_{T_q}$ denotes the contribution of the (light) quarks $q \in \{u, d, s\}$ to the mass m_N of the nucleon N.[7]

Further $\alpha_S = \frac{g_S^2}{4\pi}$, g_S denotes gauge coupling for the strong interaction; $m_{\tilde{q}_j}$ and $C^i_{\tilde{q}_j}$ denote the mass of the jth squark and its coupling with the ith (CP-even) neutral Higgs boson, respectively. The heavy quarks ($\{c, b, t\}$) contribute to f_N through the loop-induced interactions with gluons. In Eq. (23), the first term includes a contribution from the effective neutralino-quark interactions; the second and the third term includes the contributions from the effective interaction with the gluon fraction. In particular, the second term (proportional to $f^N_{T_G}\frac{\lambda^H_q}{m_q}$) and the third term (proportional to $f^N_{T_G} m_N T_{\tilde{q}}$) include the relevant contributions from the heavy quarks and all the squarks to the Higgs bosons-gluon effective vertices, respectively.

A brief discussion on various other important contributions to the DM-nucleon scattering is in order. In addition to the contribution from the Higgs boson exchange processes, there are tree-level contributions to f_N from squark exchange processes. As already mentioned, in the present discussion we assume the (first two generations of) squarks to be very heavy. In such a scenario, the dominant contribution to the spin-independent neutralino-nucleon interaction is mediated by the Higgs bosons. Further, the contribution to $f^{(H)}_N$ from the term proportional to $T_{\tilde{q}}$, which incorporates the squark contributions to the effective vertices involving Higgs bosons and gluons, is suppressed for heavy squark masses. In the present context, the only the third-generation squarks are relatively light, around 1.5 TeV. Regarding other important radiative corrections, the supersymmetric-QCD corrections to the Higgs and the down-type quark vertices [100]; the one-loop corrections to the neutralino-gluon interactions originating from the triangle vertex corrections involving (s)quarks at the Higgs-gluon-gluon vertex, and also the box diagrams involving (s)quarks can be sizable [92]. These contributions have been implemented in the numerical package micrOMEGAs [91] following Ref. [92].[8] Further, contributions from the box diagrams to the DM-quark scattering involving electroweak gauge bosons have been considered in the literature [48–50]. In Ref. [50], it has been shown that the tree-level Higgs boson exchange contribution to the (Higgsino-like) neutralino-nucleon scattering dominates over these contributions when the gaugino mass parameters are less than $\mathcal{O}(5\text{–}10)$ TeV, as is relevant in the present context.

As is evident from the discussion above, the interaction rate is proportional to f^2_N, which involves the square of the LSP-Higgs bosons vertices C_i. As discussed above, several dominant one-loop contributions to the scattering process have been estimated and incorporated in the publicly available packages, e.g., micrOMEGAs [91,101,102]. However, a detailed estimation of the one-loop corrections from the modification of the neutralino-Higgs boson vertices C_i have not received adequate attention.[9] In particular, for an almost pure Higgsino-like LSP, which is often relevant for a natural supersymmetric spectrum, the small (but generally nonvanishing) gaugino fractions imply that the tree-level value of C_i to be small. Therefore, radiative corrections to the same vertices can play a crucial role in the estimation of the cross section. In Fig. 1, some of the important diagrams contributing to the vertex correction have been depicted. We consider all the triangle diagrams involving charginos, neutralinos, gauge bosons, and Higgs bosons which contribute to the vertex corrections to the $\tilde{\chi}_1 - \tilde{\chi}_1 - h_i$ vertices. Further, as the Yukawa couplings for the third-generation (s)quarks are large, contributions from the third-generation (s)quarks have also been considered. As the loop diagrams with two fermions and one boson are generally UV divergent, we have included the vertex counterterms, and ensured the UV finiteness of the overall contributions. Note that the wave function renormalization counterterms also include the effect of mixing of the tree-level fields (due to radiative corrections from the two-point functions) appearing in the external lines. The complete set of radiative contributions considered in this work have been described in Appendix B, and the counterterms have been mentioned in Appendix C.

IV. RESULTS

In this section, we present the results highlighting the importance of the radiative corrections to the vertices involving neutralino and Higgs bosons, as discussed in Sec. III, to the (spin-independent) direct detection process in the context of a Higgsino-like $\tilde{\chi}^0_1$.

[7]We have used the scalar coefficients for the quark content in the nucleons as implemented in micrOMEGAs [97], where the mass ratios of the light quarks have been estimated using chiral perturbation theory, see, e.g., [98]. For a discussion on hadronic uncertainties in the DM-nucleus scattering cross section, see, e.g., [99].

[8]Note that, for our benchmark scenarios, all the relevant tree-level processes, including the squark exchange processes, and the radiative corrections mentioned above, have also been considered; we have used micrOMEGAs for the same. However, the percentage change in the scattering cross section has been estimated for the vertex corrections to C_i. For the radiative corrections implemented, as described above, we have checked that the contributions are about 10% to the spin-independent cross section for the benchmark scenarios.

[9]Certain subsets of the diagrams have been considered in Refs. [47–50] in the limit of a pure Higgsino or Higgsino-like neutralino DM; a full calculation of the vertex corrections, involving the respective counterterms, is not available in the literature to our knowledge.

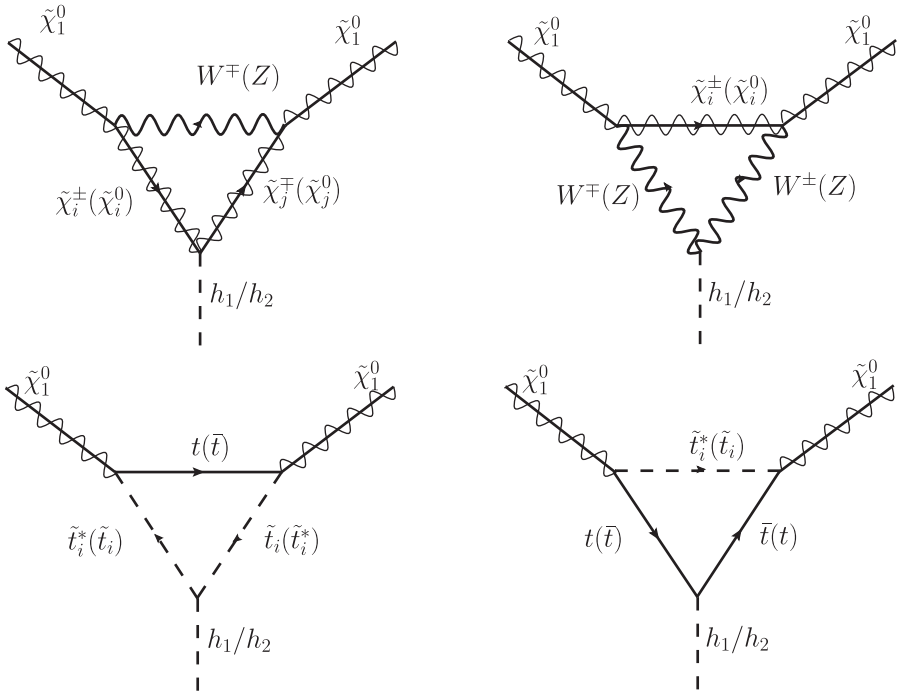

FIG. 1. Some important contributions to the $\tilde{\chi}_1^0 - \tilde{\chi}_1^0 - h_i$ vertices at one-loop level.

A. Implementation

We begin by describing the procedure to compute the radiative corrections. The steps have been sketched in the flowchart shown in Fig. 2:

(i) We generated the benchmark scenarios using the spectrum generator SPheno [103] (version 4.0.4). The parameters are read from the output file and the relevant radiative corrections are numerically evaluated using those parameters. The input parameters M_1, M_2, and μ in the chargino-neutralino sector are varied to obtain different benchmark scenarios, as presented in Tables I and II. The details of the benchmark scenarios will be discussed in the next subsection.

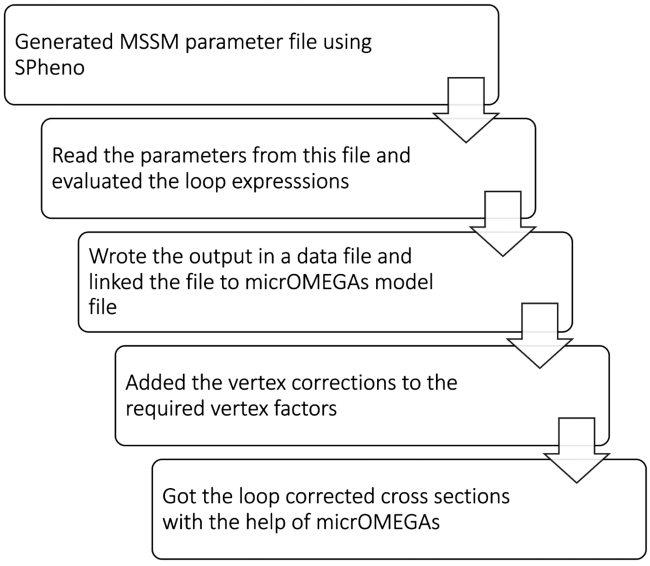

FIG. 2. The flowchart for implementation of the relevant corrections to the neutralino-Higgs boson(s) vertices.

(ii) To evaluate the radiative corrections to the $\tilde{\chi}_1^0 - \tilde{\chi}_1^0 - h_i$ vertices, we have used the publicly available packages FeynArts (version 3.11) [104,105], FormCalc (version 9.10) [106], and LoopTools (version 2.15) [106]. In particular, the Feynman diagrams are evaluated using FeynArts, and the vertex corrections are calculated using FormCalc. Further, the radiative contributions are expressed in terms of the Passarino-Veltman integrals (briefly discussed in Appendix A) and numerically evaluated for the benchmark scenarios using FormCalc and LoopTools. Further, the UV finiteness of the radiatively corrected vertex factors (including the counterterm contributions) have been numerically checked using the packages mentioned above. Finally, the numerical results are stored in data files. To determine the relevant counterterms, we have used the on shell renormalization scheme. We have used the relevant counterterms implemented in FormCalc, as described in Ref. [107].

(iii) To evaluate the direct detection cross sections micrOMEGAs [91,101,108,109] (version 5.2.1) [102] has been used. We generated the model files for micrOMEGAs using SARAH (version 4.14.5) package [110] on the Mathematica platform. We

TABLE I. The benchmark scenarios with a Higgsino-like $\tilde{\chi}_1^0$ have been tabulated for $|\mu| = 300$ GeV. HF stands for Higgsino fraction. The fixed input parameters are: the mass of the pseudoscalar Higgs boson $m_A = 1.414$ TeV, and $\tan\beta = 10$. The gluino mass parameter $M_3 = 3$ TeV. The trilinear coupling for two stops with the Higgs boson is set as $T_t = -3$ TeV. The soft-supersymmetry-breaking mass parameters for the left-type and the right-type stop and sbottom squarks are as follows: $m_{\tilde{Q}_L} = 2.69$ TeV, $m_{\tilde{t}_R} = 2.06$ TeV and $m_{\tilde{b}_R} = 2.50$ TeV. As for the physical masses, the charged Higgs boson mass $M_{H^\pm} = 1.416$ TeV, the CP-even Higgs mixing angle $\alpha = \sin^{-1}(-0.1)$. For all the benchmarks, the third-generation squark mass and mixing parameters are taken as the lightest stop mass $\mathrm{m}_{\tilde{t}_1} = 2.05$ TeV, the heaviest stop mass $\mathrm{m}_{\tilde{t}_2} = 2.71$ TeV, the lightest sbottom mass $\mathrm{m}_{\tilde{b}_1} = 2.50$ TeV, the heaviest sbottom mass $\mathrm{m}_{\tilde{b}_2} = 2.69$ TeV.

Parameters	BP1a	BP2a	BP3a	BP4a	BP5a	BP6a
μ (GeV)	300	−300	300	−300	300	300
M_1 (GeV)	−5000	−5000	5000	5000	−4000	4000
M_2 (GeV)	4000	4000	4000	4000	5000	5000
$m_{\tilde{\chi}_1^0}$ (GeV)	299.17	299.44	298.72	299.14	299.44	298.88
$m_{\tilde{\chi}_2^0}$ (GeV)	−300.44	−300.66	−300.74	−301.11	−300.29	−300.66
$m_{\tilde{\chi}_3^0}$ (GeV)	4000	4000	4000	4000	−4000	4000
$m_{\tilde{\chi}_4^0}$ (GeV)	−5000	−5000	5000	5000	5000	5000
$m_{\tilde{\chi}_1^\pm}$ (GeV)	299.56	300.2	299.56	300.2	299.67	299.67
$m_{\tilde{\chi}_2^\pm}$ (GeV)	4000	4000	4000	4000	5000	5000
m_{h_1} (GeV)	122.92	122.79	122.73	122.61	122.81	122.65
m_{h_2} (GeV)	1386	1468	1407	1448	1425	1450
HF	0.9997	0.9998	0.9997	0.9998	0.9998	0.9998
$N_{11}(\times 10^{-3})$	−6.291	−5.145	7.087	5.795	−7.756	−9.004
$N_{12}(\times 10^{-2})$	−1.679	−1.373	−1.677	−1.372	−1.322	1.321
N_{13}	0.708	−0.707	0.708	−0.708	0.708	−0.708
N_{14}	−0.706	−0.706	−0.706	−0.706	−0.706	0.706

modify the relevant vertices in the code to include the radiatively corrected vertices. For each benchmark, then, the corrected vertices are read from the output file, as described above, using a subroutine. Thus, the radiatively corrected vertices are used to evaluate the spin-independent direct detection cross section.

B. Benchmark scenarios

In this subsection, the benchmark scenarios have been discussed. The benchmark points have been described in Tables I and II.

As we focus on the Higgsino-like $\tilde{\chi}_1^0$ DM, $|\mu| \ll |M_1|, M_2$ have been set for all the benchmark scenarios. The tree-level vertices $\mathcal{C}_i^{L/R}$, as described in Eq. (14), are proportional to the product of the gaugino and Higgsino components of $\tilde{\chi}_1^0$. Thus, the tree-level spin-independent cross section (σ_{SI}) is sensitive to the variation in the gaugino-Higgsino mixing. With $|M_1|, M_2$, and $|\mu|$ fixed, the gaugino-Higgsino mixing is sensitive to the signs of M_1 and μ. Consequently, the tree-level spin-independent cross sections and the relative contributions from the radiative corrections to the $\tilde{\chi}_1^0 - \tilde{\chi}_1^0 - h_i$ vertex factors can be very different even for very similar chargino-neutralino masses. In the benchmark scenarios, with $|\mu| \ll |M_1|, M_2$; we have varied the sign of μ and M_1 to illustrate this variation. Further, the order of M_1 and M_2 have been altered to study the effect of the variation in the gaugino components.

The benchmark points BP-1a to BP-6a, as shown in Table I reflect scenarios with $|\mu| = 300$ GeV. Setting $|M_1|, M_2 \gg |\mu|$ ensures that $\tilde{\chi}_1^0, \tilde{\chi}_2^0, \tilde{\chi}_1^\pm$ are closely spaced and are Higgsino-like states. For the benchmark scenarios BP-1b to BP-6b, as shown in Table II, a heavier $|\mu| = 600$ GeV has been considered. As discussed above, to illustrate the variation in the gaugino components of $\tilde{\chi}_1^0$ for very similar particle spectra, the sign of μ and the sign of M_1 have been varied. For BP-1a and 2a, with $\mu = 300$ GeV and $\mu = -300$ GeV, respectively, M_1 is set to -5 TeV. For BP-3a and 4a, with $\mu = 300$ GeV and $\mu = -300$ GeV, respectively, M_1 is set to 5 TeV. For all these benchmark scenarios, we fix $M_2 = 4$ TeV. For BP-5a and 6a, with $\mu = 300$ GeV and $M_2 = 5$ TeV, while M_1 assumes -4 TeV and 4 TeV, respectively. BP-1b to BP-6b resembles BP-1a to BP-6a, respectively, only with $|\mu| = 600$ GeV. Note that for BP-1 to BP-4 (a and b), $|M_1| > M_2$, while for BP-5 and BP-6 (a and b) $|M_1| < M_2$. For all these benchmark scenarios $\tan\beta = 10$, the masses of the Higgs bosons and the third-generation squarks, which are also relevant

TABLE II. The benchmark scenarios with a Higgsino-like $\tilde{\chi}_1^0$ have been tabulated for $|\mu| = 600$ GeV. HF stands for Higgsino fraction. The fixed input parameters are: the mass of the pseudoscalar Higgs boson $m_A = 1.414$ TeV, and $\tan\beta = 10$. The gluino mass parameter $M_3 = 3$ TeV. The trilinear coupling for two stops with the Higgs boson is set as $T_t = -3$ TeV. The soft-supersymmetry-breaking mass parameters for the left-type and the right-type stop and sbottom squarks are $m_{\tilde{Q}_L} = 2.69$ TeV, $m_{\tilde{t}_R} = 2.06$ TeV, and $m_{\tilde{b}_R} = 2.50$ TeV. As for the physical masses, the charged Higgs boson mass $M_{H^\pm} = 1.416$ TeV, the CP-even Higgs mixing angle $\alpha = \sin^{-1}(-0.1)$. For all the benchmarks, the third-generation squark mass and mixing parameters are taken as the lightest stop mass $\mathrm{m}_{\tilde{t}_1} = 2.05$ TeV, the heaviest stop mass $\mathrm{m}_{\tilde{t}_2} = 2.71$ TeV, the lightest sbottom mass $\mathrm{m}_{\tilde{b}_1} = 2.50$ TeV, the heaviest sbottom mass $\mathrm{m}_{\tilde{b}_2} = 2.69$ TeV.

Parameters	BP1b	BP2b	BP3b	BP4b	BP5b	BP6b
μ (GeV)	600	−600	600	−600	600	600
M_1 (GeV)	−5000	−5000	5000	5000	−4000	4000
M_2 (GeV)	4000	4000	4000	4000	5000	5000
$m_{\tilde{\chi}_1^0}$ (GeV)	599.06	599.37	598.61	599.07	599.36	598.79
$m_{\tilde{\chi}_2^0}$ (GeV)	−600.39	−600.59	−600.7	−601.04	−600.24	−600.62
$m_{\tilde{\chi}_3^0}$ (GeV)	4000	4000	4000	4000	−4000	4000
$m_{\tilde{\chi}_4^0}$ (GeV)	−5000	−5000	−5000	5000	5000	5000
$m_{\tilde{\chi}_1^\pm}$ (GeV)	599.43	600.08	599.43	600.08	599.58	599.58
$m_{\tilde{\chi}_2^\pm}$ (GeV)	4000	4000	4000	4000	5000	5000
m_{h_1} (GeV)	122.94	122.68	122.75	122.51	122.83	122.65
m_{h_2} (GeV)	1347	1506	1390	1465	1423	1450
HF	0.9997	0.9998	0.9996	0.9997	0.9997	0.9997
$N_{11}(\times 10^{-3})$	5.956	−4.872	−7.575	−6.196	−7.252	−9.804
$N_{12}(\times 10^{-2})$	1.827	−1.495	1.827	1.494	−1.412	1.412
N_{13}	−0.707	−0.707	−0.708	0.708	0.707	−0.708
N_{14}	0.707	−0.707	0.706	0.706	−0.707	0.706

for the present study, have been kept fixed. Further, constraints from LHC on such compressed spectra have been taken into account.

For all the benchmark scenarios, $\tilde{\chi}_1^0$ corresponds to a mass eigenstate with positive eigenvalue. In the benchmark scenarios with a negative μ parameter, i.e. BP-2a, BP-2b, BP-4a, and BP-4b, $\tilde{\chi}_1^0$ is the symmetric Higgsino-like state. For all other benchmarks (with positive μ parameter) $\tilde{\chi}_1^0$ is the antisymmetric Higgsino-like state. Note that, irrespective of the sign of M_1, the gaugino components in $\tilde{\chi}_1^0$ are reduced substantially for negative μ (where $\tilde{\chi}_1^0$ is the symmetric state) as compared to positive μ (where $\tilde{\chi}_1^0$ is the symmetric state). This is evident from comparing the wino and the bino components (N_{12}, N_{11}, respectively) of $\tilde{\chi}_1^0$ in BP-1a(b) and BP-2a(b), respectively. In particular, the wino component is reduced by approximately 50% and 25% for benchmarks BP-1a(b) and BP-2a(b), respectively. The bino content, which contributes subdominantly, follows a similar trend, although by a smaller margin. As the tree-level $\tilde{\chi}_1^0 - \tilde{\chi}_1^0 - h_i$ vertices are directly proportional to the gaugino fraction, the change in sign of the Higgsino mass parameter μ leads to a significant change in the tree-level spin-independent direct detection cross section.

C. Numerical results and discussion

In this section, we discuss the numerical results. The radiative corrections to the $\tilde{\chi}_1^0 - \tilde{\chi}_1^0 - h_i$ vertices for the benchmark scenarios, as described in Tables I and II, have been computed and have been presented in Table III. In Table III, the one-loop corrected $\tilde{\chi}_1^0 - \tilde{\chi}_1^0 - h_i$ vertices ($\mathcal{C}_i^{L/R}$) for the respective benchmark scenarios (as mentioned in the first column) have been presented in the second column. In the third and the fourth column the percentage contribution from the radiative corrections to the $\tilde{\chi}_1^0$-proton spin-independent scattering cross sections $\Delta\mathcal{C}_i^{L/R} = \frac{\mathcal{C}_i^{L/R} - \mathcal{C}_{i\,\mathrm{tree}}^{L/R}}{\mathcal{C}_{i\,\mathrm{tree}}^{L/R}} \times 100\%$ have been described for $i = 1$ and $i = 2$, respectively. Note that in the present scenario, the results are similar for $\tilde{\chi}_1^0$-neutron spin-independent scattering cross sections. For estimating the radiative corrections, contributions from the loops involving all the neutralinos and charginos, gauge bosons, Higgs bosons, and third-generation (s)quarks have been considered. Individual contributions from all the loops, counterterms, and also the third-generation (s)quarks to the respective vertices have been mentioned. Finally, the radiatively corrected $\tilde{\chi}_1^0$–nucleon cross section and the percentage contribution to the same $\Delta\sigma_{\mathrm{SI}} = \frac{\sigma_{\mathrm{SI}} - \sigma_{\mathrm{SI\,tree}}}{\sigma_{\mathrm{SI\,tree}}} \times 100\%$ are

TABLE III. $\Delta\mathcal{C}_i^{L/R}$ (%) denotes the percentage correction to the $\tilde{\chi}_1^0 - \tilde{\chi}_1^0 - h_i$ vertices $\mathcal{C}_i^{L/R}$. $\sigma_{\rm SI}$ denotes spin-independent cross section (with proton) including the radiative corrections and $\Delta\sigma_{\rm SI}$ (%) denotes the percentage contribution to the same from the radiative corrections under consideration. In the third and the fourth column title, "Total" refers to total percentage correction to $\mathcal{C}_i^{L/R}$, "CT" refers to the percentage contribution from the counterterm vertex, "Loop" denotes the percentage contribution from the one-loop diagrams, and "SQ" denotes the percentage contribution from the third-generation quarks and squarks running in the loops.

BP	$\mathcal{C}_1^{L/R}$, $\mathcal{C}_2^{L/R}$	$\Delta\mathcal{C}_1^{L/R}$ (%) Total (SQ) (Loop, CT)	$\Delta\mathcal{C}_2^{L/R}$ (%) Total (SQ) (Loop, CT)	$\sigma_{\rm SI}$ [pb] ($\Delta\sigma_{\rm SI}$ %)
BP1a	7.96×10^{-3} 4.68×10^{-3}	19.74(−22.35) (2.74, 17.0)	−13.96(−2.9) (−17.63, 3.67)	4.13×10^{-11} (41.7)
BP1b	8.64×10^{-3} 5.24×10^{-3}	15.50(−26.62) (−1.52, 17.03)	−14.29(−1.02) (−18.0, 3.74)	4.89×10^{-11} (31.5)
BP2a	6.12×10^{-3} -4.36×10^{-3}	37.88(−29.52) (20.89, 16.99)	−19.87(−9.05) (−23.53, 3.66)	2.29×10^{-11} (96)
BP2b	6.63×10^{-3} -4.82×10^{-3}	32.7(−35.78) (15.73, 16.97)	−21.22(−8.18) (−25, 3.78)	2.71×10^{-11} (81)
BP3a	1.13×10^{-2} 7.77×10^{-3}	11.07(−18.05) (−7.1, 18.2)	−6.98(−1.39) (−11.83, 4.89)	8.46×10^{-11} (22.4)
BP3b	1.21×10^{-2} 8.37×10^{-3}	9.14(−21.22) (−9.13, 18.27)	−7.63(−0.26) (−12.66, 5.03)	9.67×10^{-11} (18.25)
BP4a	8.25×10^{-3} -7.33×10^{-3}	21.11(−24.33) (2.81, 18.3)	−12.36(−6.99) (−17.31, 4.95)	4.13×10^{-11} (49.75)
BP4b	8.82×10^{-3} -7.83×10^{-3}	19.21(−28.89) (0.87, 18.34)	−13.74(−6.57) (−18.83, 5.09)	4.77×10^{-11} (45)
BP5a	6.24×10^{-3} 3.06×10^{-3}	38.95(−25.5) (22.47, 16.48)	−16.6(−2.68) (−20.35, 3.75)	2.53×10^{-11} (89.6)
BP5b	6.74×10^{-3} 3.49×10^{-3}	32.88(−31.58) (16.27, 16.61)	−15.77(−0.26) (−19.72, 3.95)	2.97×10^{-11} (73.8)
BP6a	1.05×10^{-2} 6.94×10^{-3}	17.0(−17.81) (−1.42, 18.42)	−5.32(−0.65) (−10.42, 5.10)	7.26×10^{-11} (35.8)
BP6b	1.11×10^{-2} 7.43×10^{-3}	15.41(−21.43) (−3.20, 18.61)	−5.44(−0.74) (−10.8, 5.36)	8.13×10^{-11} (32.2)

presented in the fifth column. In the above discussion, the subscript "tree" denotes the respective quantities without including the radiative corrections considered in this article. As discussed in the previous section, we have used FeynArts, FormCalc, and LoopTools for the numerical evaluation of the radiative contributions and the relevant counterterms.

As described in Tables I and II, for all the benchmark scenarios $\tilde{\chi}_1^0$ is dominantly Higgsino-like. The Higgsino fraction (HF $= |N_{13}|^2 + |N_{14}|^2$) is above 99%. The radiative corrections to the $\tilde{\chi}_1^0 - \tilde{\chi}_1^0 - h_1$ vertex $\mathcal{C}_1^{L/R}$ contributes dominantly to the spin-independent cross section $\sigma_{\rm SI}$. The contribution to the spin-independent cross section $\sigma_{\rm SI}$ from the heavy Higgs boson h_2 is only about $\lesssim$3% for all the benchmark scenarios. This is because $m_{h_2} \gg m_{h_1}$ (about ten times) in the present context. Therefore, its contribution to the $\tilde{\chi}_1^0$- nucleon coupling λ_q^H ($\propto \frac{1}{m_{h_2}^2}$) is suppressed, as can be inferred from Eq. (22). Thus, for all the benchmark scenarios, the percentage corrections to the cross section $\sigma_{\rm SI}$ are approximately twice that of the percentage corrections to the $\tilde{\chi}_1^0 - \tilde{\chi}_1^0 - h_1$ vertex factor $\mathcal{C}_1^{L/R}$.

The radiative corrections to $\tilde{\chi}_1^0 - \tilde{\chi}_1^0 - h_1/h_2$ vertices are significant for all the benchmark scenarios and vary between approximately 9%-40% for the light Higgs boson vertex and between approximately 5%-21% for the vertex involving the heavy Higgs boson. Comparing the first eight benchmarks (BP-1a to BP-4b), the percentage change in the $\tilde{\chi}_1^0 - \tilde{\chi}_1^0 - h_1$ vertices are significant for the benchmarks with negative μ (BP-2a, BP-2b and BP-4a, BP-4b), as compared to their counterparts with positive μ (BP-1a,

BP-1b and BP-3a, BP-3b). Let us consider BP-1a(b) and BP-2a(b). While BP-1a(b) and BP-2a(b) only differ by the sign of μ, thus, the percentage contribution to $\mathcal{C}_1^{L/R}$ from the radiative correction for BP-2a(b) is significantly higher as compared to BP-1a(b). This is largely because of a substantial reduction in the tree-level vertex factor for BP-2a and BP-2b, while the radiative corrections are also marginally higher. Note that, for positive (negative) μ, $\tilde{\chi}_1^0$ is the symmetric (antisymmetric) Higgsino-like state. A similar argument explains the larger percentage corrections in the context of BP-4a(b), as compared to BP-3a(b). It follows from Eq. (14), that for the symmetric states, the respective tree-level vertex suffers from cancellation between two terms proportional to N_{13} and N_{14}, respectively. In all the benchmark scenarios, the dominant loop contributions to $\mathcal{C}_1^{L/R}$ come from the triangle loops involving two vector bosons and one neutralino/chargino. Further, the third-generation (s)quarks contribute significantly thanks to the large Yukawa couplings. The contributions from the loops involving, in particular, two quarks and one squark tend to negate the contributions from the loops involving the vector bosons and one neutralino/ chargino. In BP-5a(b) and BP-6a(b), the difference in the percentage contribution to $\mathcal{C}_1^{L/R}$ is largely attributed to the cancellation from the (s) quark loop. Further, contributions from the vertex counterterms are substantial. In particular, we find sizable contributions from the terms proportional to the diagonal and off-diagonal wave-function renormalization counterterms.

The vertex counterterms are evaluated following the implementation in FormCalc [107]. The details have been discussed in Appendix C. On shell renormalization schemes have been adopted for the neutralino-chargino sector [73]. In particular, for BP1a to BP-4b, two chargino masses and the heaviest neutralino mass (CCN[4]) have been used as on shell input masses. For BP-5a, BP-5b, BP-6a, and BP-6b, two chargino masses and the third neutralino mass (CCN[3]) have been used as on shell input masses. This ensures that there is always a binolike neutralino among the input masses [74,111]. The respective contributions from the counterterms have been shown in Table III. Note that we have used tree-level masses for all the neutralinos and charginos, including $\tilde{\chi}_1^0$ for the eastimation of the spin-independent scattering cross section. This ensures that the percentage corrections to the cross section reflects only the contributions from the vertex corrections, which we intend to illustrate.

As the spin-independent cross section of $\tilde{\chi}_1^0$ with the nucleons (protons and neutrons) receive dominant contributions from the light Higgs boson-mediated processes, the percentage corrections to the cross sections about twice the respective percentage corrections to the $\tilde{\chi}_1^0 - \tilde{\chi}_1^0 - h_1$ vertex. These cross sections can be enhanced by up to about 100% for the benchmark scenarios. This highlights the importance of these corrections in the present context.

Note that, as mentioned in Sec. I and elaborated further in Sec. III, certain important loop corrections to the Higgs bosons-nucleon interactions, which contribute to the effective neutralino-nucleon effective operators [see Eqs. (20) and (21)], have been already included in micrOMEGAs. Thus, the cross sections computed using the one-loop corrections to $\tilde{\chi}_1^0 - \tilde{\chi}_1^0 - h_1/h_2$ vertices also effectively include certain two-loop contributions. These corrections are also included in the cross sections with which we have compared the final results after including the vertex corrections. Thus, the percentage corrections to the cross sections, as mentioned in Sec. III, solely come from the corrections to the $\tilde{\chi}_1^0 - \tilde{\chi}_1^0 - h_1/h_2$ vertices.

Assuming that $\tilde{\chi}_1^0$ constitutes the entirety of DM, we have further considered the implications of these large corrections for the viability of sub-TeV Higgsino-like DM in light of stringent limits from the direct detection experiments. We consider the DM-nucleon (proton) cross section limits from the LUX-ZEPLIN (LZ) experiment [37] and compare the status of the benchmark scenarios after including the radiative corrections as shown in Fig. 3(a). We find that, thanks to the radiative corrections, benchmark point BP-1a is pushed above the lower limit of the 1σ sensitivity band (dotted line), and BP-1b is pushed close to the 1σ band. Benchmark points BP-2a and BP-2b are pushed close to the 1σ band while lying below it. The benchmark BP-3a falls on the exclusion line (solid line) and is close to being ruled out after the corrections are added, and BP-3b is also close to the exclusion limit. As for benchmark BP4a, it is pushed above the 1σ lower band, and BP-4b is pushed close to it. BP-5a and BP-5b are also pushed closer to the 1σ band of the exclusion region; finally, BP6a and BP6b benchmarks are pushed above the 1σ band and close to the exclusion limit when the corrections are added. Although, to estimate the overall impact on the scattering cross section all the radiative corrections need to be considered together, the above discussion aims to demonstrate the relative importance of the vertex corrections, in comparison with the same cross section evaluated using the tree-level vertices C_i.[10] To demonstrate the significance of the radiative corrections on constraining the Higgsino mass parameter μ in the

[10]Note that by changing the stop-stop-Higgs boson soft-supersymmetry-breaking trilinear term T_t to -4 TeV, the light Higgs mass m_{h_1}, as computed by SPheno, becomes about 125 GeV. We have checked that using $m_{h_1} \simeq 125$ GeV, with the above modifications to the stop sector parameters, does not affect the vertex corrections and the percentage corrections to the direct detection cross section appreciably. For most of the benchmark scenarios, which assume $m_{h_1} \simeq 123$ GeV, using the parameters as mentioned above lead to variations in the percentage correction to the neutralino-proton cross section ($\Delta\sigma_{\rm SI}$) by less than ~3%. Further, note that while using $m_{h_1} \simeq 125$ GeV, keeping all the other parameters as the benchmark scenarios, does not change in the vertex corrections appreciably, and thus, the percentage change in the spin-independent cross sections ($\Delta\sigma_{\rm SI}$) are also well below a percent.

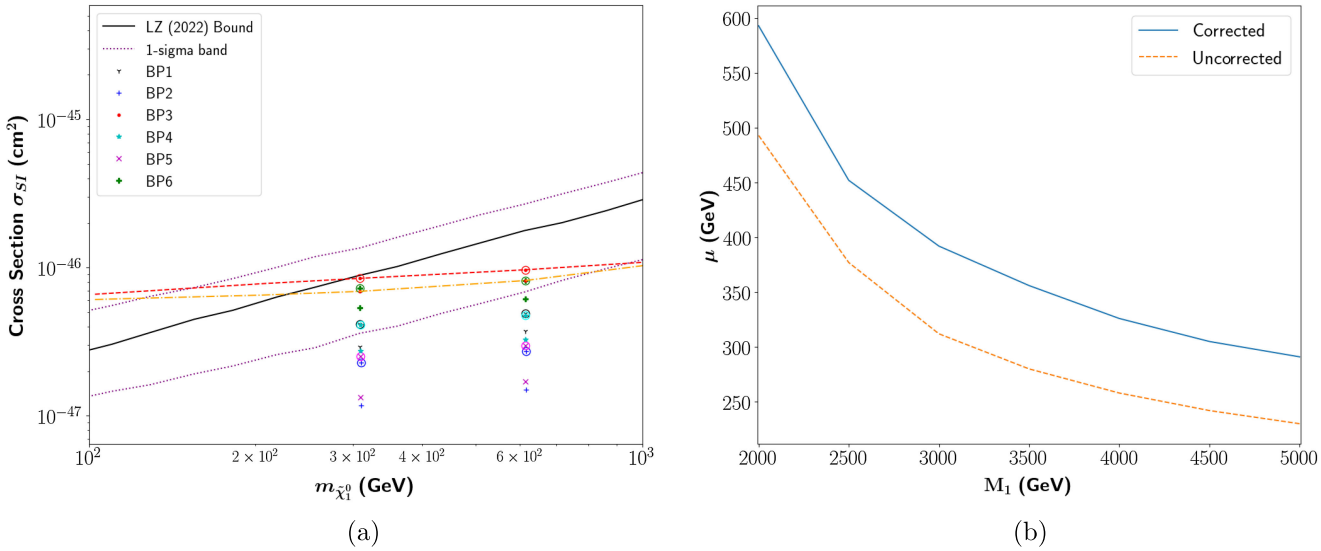

FIG. 3. Panel (a) shows the comparison of the shift of various benchmark points (Table III) before and after adding the vertex corrections ($\mathcal{C}_i^{L/R}$) with the direct detection bound of LUX-ZEPLIN (LZ) experiment [37]. The circled points depict the corrected cross sections ($\sigma_{\rm SI}$) and the uncircled ones are without the corrections ($\sigma_{\rm SI\ tree}$). Panel (b) shows the shift in the μ parameter for different values of M_1 as constrained by LZ (2022) [37] after adding the vertex corrections ($\mathcal{C}_i^{L/R}$). The change in the constraint on the μ parameter (for $\mu \ll M_1, M_2$) corresponding to the cross section after adding the vertex corrections $\mathcal{C}_i^{L/R}$ is shown by the solid line, the dashed line represents the case without the corrections ($\mathcal{C}_{i\rm tree}^{L/R}$). Here, M_2 is taken as 4 TeV and the other parameters are assumed to be the same as mentioned in Table I.

present context, we further vary the μ parameter keeping all the other relevant parameters the same as BP-3a(or b). The cross sections with the radiatively corrected $\tilde{\chi}_1^0 - \tilde{\chi}_1^0 - h_1/h_2$ vertices ($\mathcal{C}_i^{L/R}$) and the respective tree-level vertices ($\mathcal{C}_{i\rm tree}^{L/R}$) have been used to obtain the dashed red line and the dot-dashed orange line respectively in Fig. 3(a). As demonstrated in the figure, the dashed red line intersects the 90% confidence limit from the LZ experiment [37] for a heavier $m_{\tilde{\chi}_1^0}$, as compared to the dot-dashed orange line. As in the present context $m_{\tilde{\chi}_1^0} \simeq |\mu|$ (as $|\mu| \ll |M_1|, M_2$), therefore, the constraint on the μ parameter is improved. This is further illustrated in Fig. 3(b) with positive M_1 and $\mu(\mu \ll M_1, M_2)$. In this figure, the constraint on μ parameter is shown to vary with respect to M_1. We have assumed, as in the benchmark scenarios, $\tan\beta = 10, M_2 = 4$ TeV and $M_A = 1.414$ TeV; the other parameters are also kept the same as mentioned in Tables I and II. As shown in Fig. 3(b), for $M_1 = 2$ TeV, $\mu \lesssim 493$ GeV (as shown by the dashed line) is excluded by the direct detection experiment LZ, when tree-level $\tilde{\chi}_1^0 - \tilde{\chi}_1^0 - h_1/h_2$ vertices are used to estimate the respective cross sections. While estimating the cross-section using the radiatively corrected vertices ($\mathcal{C}_i^{L/R}$), the constraint shifts to $\mu \lesssim 593$ GeV (as shown by the solid line), a shift of 100 GeV. Likewise, the bound on μ shifts from 230 to 291 GeV for $M_1 = 5$ TeV. Thus, the constraint on the μ parameter space (with $\mu \ll M_1,\ M_2$) becomes more stringent by about 60–100 GeV, as illustrated in this figure.[11]

V. CONCLUSION

Light Higgsino-like $\tilde{\chi}_1^0$ fits well within the framework of natural supersymmetry. In this article, we have considered Higgsino-like $\tilde{\chi}_1^0$ DM within R-parity conserving MSSM and have studied the importance of a class of radiative corrections to the $\tilde{\chi}_1^0 - \tilde{\chi}_1^0 - h_1/h_2$ vertices in the context of spin-independent direct detection. The tree-level couplings between $\tilde{\chi}_1^0$ and the CP-even neutral Higgs bosons (h_1, h_2), in such a scenario, are suppressed by small gaugino-Higgsino mixing. However, as demonstrated in this article, the radiative contributions to these vertices (including the respective counterterms) from the loops involving the charginos, neutralinos, gauge bosons, and Higgs bosons can have significant implications for direct detection. Further, third-generation (s)quark contributions are significant and tend to cancel the former to some extent in the parameter region considered in this article. For the benchmark scenarios presented, the radiatively corrected vertices can be enhanced by about 40% compared to the respective

[11]The cases for other combinations of signs of M_1 and μ are not shown as their cross sections lie below the LZ bounds in the parameter space of our interest.

tree-level vertices. The spin-independent cross section of $\tilde{\chi}_1^0$ with the nucleons (protons and neutrons), which receives a significant contribution from the CP-even neutral Higgs boson mediated processes through the respective effective operators, thus, can be enhanced by about 100% in certain benchmark scenarios. We further illustrate that the corrections are sensitive to the sign of μ and the choice of the gaugino mass parameters M_1 and M_2, even though $|\mu| \ll |M_1|, M_2$. Note that, the "tree-level" cross section in such scenarios is quite sensitive to the small gaugino admixture in the $\tilde{\chi}_1^0$. Thus, generally, the constraint on the mass of sub-TeV Higgsino-like $\tilde{\chi}_1^0$, after including these corrections, is sensitive to the sign of μ and the choice of the gaugino mass parameters M_1 and M_2. As mentioned in the Introduction, in the sub-TeV mass region, the thermal relic abundance of a Higgsino-like $\tilde{\chi}_1^0$ LSP is inadequate to fulfill the required relic abundance of DM ($\Omega_{\rm DM}h^2 = 0.12$ [60]). Thus, assuming only thermal production of $\tilde{\chi}_1^0$ will lead to a dilution of the direct detection constraints on $\tilde{\chi}_1^0$, in proportion to the relative abundance of $\tilde{\chi}_1^0$. However, considering the possibility of nonthermal production of $\tilde{\chi}_1^0$ in the early Universe, there is a possibility that $\tilde{\chi}_1^0$ constitutes the entire DM. In any scenario, the result demonstrates the significance of the complete vertex corrections to the $\tilde{\chi}_1^0 - \tilde{\chi}_1^0 - h_1/h_2$ vertices in the spin-independent scattering cross section of a Higgsino-like $\tilde{\chi}_1^0$ DM.

ACKNOWLEDGMENTS

The authors thank B. De for his contributions in the early stages of this work. We acknowledge useful discussions with S. Heinemeyer, A. Pukhov, and C. Schappacher. A. C. acknowledges the hospitality at IoP, Bhubaneswar, during the meeting IMHEP-19 and IMHEP-22 which facilitated this work. A. C. and S. A. P. also acknowledge the hospitality at IoP, Bhubaneswar, during a visit. S. B. acknowledges the local hospitality at SNIoE, Greater Noida, during the meeting at WPAC-2023 where this work was finalized.

APPENDIX A

In this appendix, we summarize the Passarino-Veltman functions [112], which appear in the radiative corrections, as described in Appendix B. We follow the convention of Refs. [113,114]. The Passarino-Veltman C functions have the following form:

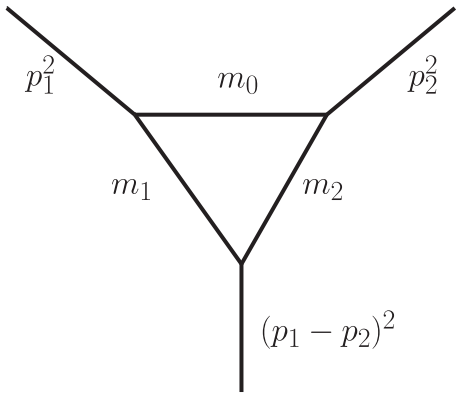

FIG. 4. The above figure shows the mass and momentum convention for the Passarino-Veltman functions.

$$\begin{aligned}&\mathbf{C}_0(p_1^2,(p_1-p_2)^2,p_2^2,m_0,m_1,m_2)\\&= -\int_0^1 \mathrm{d}x \int_0^{1-x} \mathrm{d}y[x^2p_1^2 + y^2p_2^2 + xy2p_1p_2\\&\quad - x(p_1^2 - m_1^2 + m_0^2) - y(p_2^2 - m_2^2 + m_0^2)\\&\quad + m_0^2 - i\epsilon]^{-1}. \end{aligned} \tag{A1}$$

We have used the following abbreviation:

$$\langle \cdots \rangle_q := \frac{(2\pi\tilde{\mu})^{4-D}}{i\pi^2} \int \mathrm{d}^D q \cdots, \tag{A2}$$

where $\tilde{\mu}$ denotes a parameter with dimension of mass. Further,

$$\begin{aligned}&\mathbf{C}_\mu(p_1^2,(p_1-p_2)^2,p_2^2,m_0,m_1,m_2)\\&= \left\langle \frac{q_\mu}{(q^2-m_0^2)[(q+p_1)^2-m_1^2][(q+p_2)^2-m_2^2]} \right\rangle_q\\&= p_{1,\mu}\mathbf{C}_1 + p_{2,\mu}\mathbf{C}_2. \end{aligned} \tag{A3}$$

Contraction with p_1^μ, then, gives

$$\begin{aligned}&p_1^2\mathbf{C}_1 + p_1p_2\mathbf{C}_2\\&= \left\langle \frac{\frac{1}{2}[(q+p_1)^2-m_1^2] - \frac{1}{2}(q^2-m_0^2) - \frac{1}{2}(p_1^2-m_1^2+m_0^2)}{(q^2-m_0^2)[(q+p_1)^2-m_1^2][(q+p_2)^2-m_2^2]} \right\rangle_q\\&= \frac{1}{2}\mathbf{B}_0(p_2^2,m_0,m_2) - \frac{1}{2}\mathbf{B}_0((p_1-p_2)^2,m_1,m_2)\\&\quad - \frac{1}{2}(p_1^2-m_1^2+m_0^2)\mathbf{C}_0, \end{aligned}$$

where the momenta and masses are as shown in Fig. 4. Further,

$$\begin{pmatrix}\mathbf{C}_1\\ \mathbf{C}_2\end{pmatrix} = \begin{pmatrix}p_1^2 & p_1p_2\\ p_1p_2 & p_2^2\end{pmatrix}^{-1} \cdot \begin{pmatrix}\frac{1}{2}\mathbf{B}_0(p_2^2,m_0,m_2) - \frac{1}{2}\mathbf{B}_0((p_1-p_2)^2,m_1,m_2) - \frac{1}{2}f_1\mathbf{C}_0\\ \frac{1}{2}\mathbf{B}_0(p_1^2,m_0,m_1) - \frac{1}{2}\mathbf{B}_0((p_1-p_2)^2,m_1,m_2) - \frac{1}{2}f_2\mathbf{C}_0\end{pmatrix}, \tag{A4}$$

where $f_i = p_i^2 - m_i^2 + m_0^2$, for $i \in \{1,2\}$. In the expressions above, $\mathbf{B}_0$ is given by

$$\mathbf{B}_0(p_1, m_0, m_1) = \Delta - \int_0^1 \mathrm{d}x \log\left[\frac{x^2 p_1^2 - x(p_1^2 - m_1^2 + m_0^2) + m_0^2 - i\epsilon}{\mu^2}\right] + \mathcal{O}(D-4), \tag{A5}$$

where $\Delta \coloneqq \frac{2}{4-d} - \gamma_E + \log 4\pi$, γ_E is the Euler-Mascheroni constant and d stands for space-time dimension.

APPENDIX B

In this appendix, we discuss the radiative corrections to the $\tilde{\chi}_1^0 - \tilde{\chi}_1^0 - h_i$ vertices originating from the triangle diagrams. In particular, generic expressions for contributions from scalar bosons, vector bosons, and fermions running in the loops have been provided. In the following discussion, F and F' denote fermions, S and S' are used for scalar bosons, and V denotes vector bosons. Further, q^2 denotes the square of the momentum transferred from the incident $\tilde{\chi}_1^0$ to the quarks in the nucleons, and d stands for space-time dimension. Here, G and $G^{\pm}$ refer to the neutral and charged Goldstone bosons, respectively. We have evaluated the expressions using Package-X (version 2.1.1) [113], and have also checked some of these expressions by explicit calculations. Feynman gauge has been used for the calculation. The vertices may be found in Ref. [65].

1. Topology-(1a)

The respective Feynman diagram is shown in Fig. 5(a).

$$i\delta\Gamma^{(a)} = -\frac{i}{16\pi^2}[P_L\{\xi_{LL} m_F \mathbf{C}_0 - \xi_{LR} m_{\tilde{\chi}_1^0}\mathbf{C}_1 - \xi_{RL} m_{\tilde{\chi}_1^0}\mathbf{C}_2\} + P_R\{\xi_{RR} m_F \mathbf{C}_0 - \xi_{RL} m_{\tilde{\chi}_1^0}\mathbf{C}_1 - \xi_{LR} m_{\tilde{\chi}_1^0}\mathbf{C}_2\}], \tag{B1}$$

where $\mathbf{C}_i = \mathbf{C}_i(m_{\tilde{\chi}_1^0}^2, q^2, m_{\tilde{\chi}_1^0}^2; m_F, m_S, m_S')$, and

$$\xi_{LL} = \lambda_{h_i SS'} \mathcal{G}^L_{\tilde{\chi}_1^0 FS'} \mathcal{G}^L_{\tilde{\chi}_1^0 FS}, \quad \xi_{LR} = \lambda_{h_i SS'} \mathcal{G}^L_{\tilde{\chi}_1^0 FS'} \mathcal{G}^R_{\tilde{\chi}_1^0 FS}, \tag{B2}$$

$$\xi_{RL} = \lambda_{h_i SS'} \mathcal{G}^R_{\tilde{\chi}_1^0 FS'} \mathcal{G}^L_{\tilde{\chi}_1^0 FS}, \quad \xi_{RR} = \lambda_{h_i SS'} \mathcal{G}^R_{\tilde{\chi}_1^0 FS'} \mathcal{G}^R_{\tilde{\chi}_1^0 FS}. \tag{B3}$$

(1) $h_i = h_1/h_2$, $F = \tilde{\chi}_\ell^0$, and $S = S' = h_1$.

$$\xi_{LL} = \lambda_{h_i h_1 h_1} \mathcal{G}^L_{\tilde{\chi}_1^0 \tilde{\chi}_\ell^0 h_1} \mathcal{G}^{R*}_{\tilde{\chi}_1^0 \tilde{\chi}_\ell^0 h_1}, \quad \xi_{LR} = \lambda_{h_i h_1 h_1} \mathcal{G}^L_{\tilde{\chi}_1^0 \tilde{\chi}_\ell^0 h_1} \mathcal{G}^{L*}_{\tilde{\chi}_1^0 \tilde{\chi}_\ell^0 h_1}, \tag{B4}$$

$$\xi_{RL} = \lambda_{h_i h_1 h_1} \mathcal{G}^R_{\tilde{\chi}_1^0 \tilde{\chi}_\ell^0 h_1} \mathcal{G}^{R*}_{\tilde{\chi}_1^0 \tilde{\chi}_\ell^0 h_1}, \quad \xi_{RR} = \lambda_{h_i h_1 h_1} \mathcal{G}^R_{\tilde{\chi}_1^0 \tilde{\chi}_\ell^0 h_1} \mathcal{G}^{L*}_{\tilde{\chi}_1^0 \tilde{\chi}_\ell^0 h_1}, \tag{B5}$$

where $\lambda_{h_i h_i h_i} = -3\frac{g_2 M_Z}{2c_W} B_{h_i}$, with $B_{h_i} = \{^{c_{2\alpha} s_{\beta+\alpha};\ h_i = h_1}_{c_{2\alpha} c_{\beta+\alpha};\ h_i = h_2}$,

$$\mathcal{G}^L_{\tilde{\chi}_1^0 \tilde{\chi}_\ell^0 h_i} = \begin{cases} g_2(Q''^*_{\ell 1} s_\alpha + S''^*_{\ell 1} c_\alpha); & h_i = h_1 \\ g_2(-Q''^*_{\ell 1} c_\alpha + S''^*_{\ell 1} s_\alpha); & h_i = h_2 \end{cases},$$

$$\mathcal{G}^R_{\tilde{\chi}_1^0 \tilde{\chi}_\ell^0 h_i} = \begin{cases} g_2(Q''_{1\ell} s_\alpha + S''_{1\ell} c_\alpha); & h_i = h_1 \\ g_2(-Q''_{1\ell} c_\alpha + S''_{1\ell} s_\alpha); & h_i = h_2 \end{cases}.$$

(2) $h_i = h_1/h_2$, $F = \tilde{\chi}_\ell^0$, and $S = h_1$, $S' = h_2$ or $S = h_2$, $S' = h_1$.

$$\xi_{LL} = \lambda_{h_i h_1 h_2} \mathcal{G}^L_{\tilde{\chi}_1^0 \tilde{\chi}_\ell^0 h_2} \mathcal{G}^{R*}_{\tilde{\chi}_1^0 \tilde{\chi}_\ell^0 h_1}, \quad \xi_{LR} = \lambda_{h_i h_1 h_2} \mathcal{G}^L_{\tilde{\chi}_1^0 \tilde{\chi}_\ell^0 h_2} \mathcal{G}^{L*}_{\tilde{\chi}_1^0 \tilde{\chi}_\ell^0 h_1}, \tag{B6}$$

$$\xi_{RL} = \lambda_{h_i h_1 h_2} \mathcal{G}^R_{\tilde{\chi}_1^0 \tilde{\chi}_\ell^0 h_2} \mathcal{G}^{R*}_{\tilde{\chi}_1^0 \tilde{\chi}_\ell^0 h_1}, \quad \xi_{RR} = \lambda_{h_i h_1 h_2} \mathcal{G}^R_{\tilde{\chi}_1^0 \tilde{\chi}_\ell^0 h_2} \mathcal{G}^{L*}_{\tilde{\chi}_1^0 \tilde{\chi}_\ell^0 h_1}, \tag{B7}$$

where $\lambda_{h_i h_1 h_2} = \frac{g_2 M_Z}{2c_W} C_{h_i}$, with $C_{h_i} = \{^{-2 s_{2\alpha} s_{\beta+\alpha} + c_{\beta+\alpha} c_{2\alpha};\ h_i = h_1}_{2 s_{2\alpha} c_{\beta+\alpha} + s_{\beta+\alpha} c_{2\alpha};\ h_i = h_2}$.

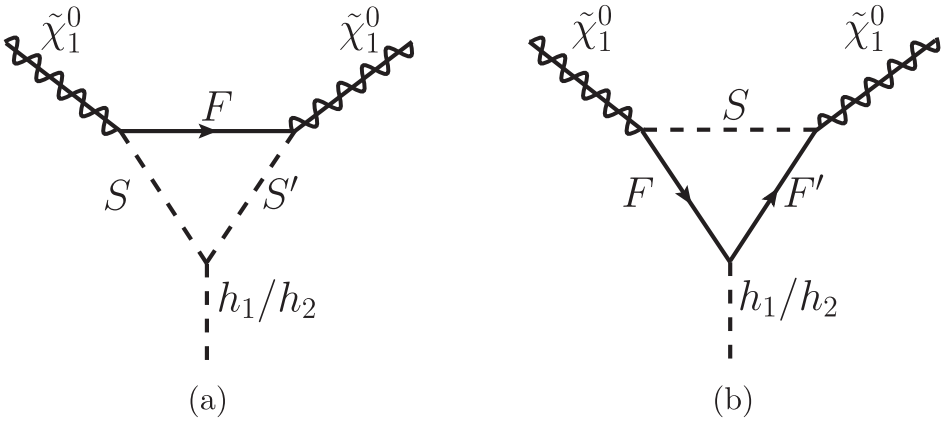

FIG. 5. Topology 1(a) and 1(b).

(3) $h_i = h_1/h_2$, $F = \tilde{\chi}^0_\ell$, and $S = S' = h_2$.

$$\xi_{LL} = \lambda_{h_i h_2 h_2} \mathcal{G}^L_{\tilde{\chi}^0_1 \tilde{\chi}^0_\ell h_2} \mathcal{G}^{R*}_{\tilde{\chi}^0_1 \tilde{\chi}^0_\ell h_2},$$
$$\xi_{LR} = \lambda_{h_i h_2 h_2} \mathcal{G}^L_{\tilde{\chi}^0_1 \tilde{\chi}^0_\ell h_2} \mathcal{G}^{L*}_{\tilde{\chi}^0_1 \tilde{\chi}^0_\ell h_2}, \tag{B8}$$

$$\xi_{RL} = \lambda_{h_i h_2 h_2} \mathcal{G}^R_{\tilde{\chi}^0_1 \tilde{\chi}^0_\ell h_2} \mathcal{G}^{R*}_{\tilde{\chi}^0_1 \tilde{\chi}^0_\ell h_2},$$
$$\xi_{RR} = \lambda_{h_i h_2 h_2} \mathcal{G}^R_{\tilde{\chi}^0_1 \tilde{\chi}^0_\ell h_2} \mathcal{G}^{L*}_{\tilde{\chi}^0_1 \tilde{\chi}^0_\ell h_2}, \tag{B9}$$

(4) $h_i = h_1/h_2$, $F = \tilde{\chi}^0_\ell$, and $S = S' = A$.

$$\xi_{LL} = \lambda_{h_i AA} \mathcal{G}^L_{\tilde{\chi}^0_1 \tilde{\chi}^0_\ell A} \mathcal{G}^{R*}_{\tilde{\chi}^0_1 \tilde{\chi}^0_\ell A},$$
$$\xi_{LR} = \lambda_{h_i AA} \mathcal{G}^L_{\tilde{\chi}^0_1 \tilde{\chi}^0_\ell A} \mathcal{G}^{L*}_{\tilde{\chi}^0_1 \tilde{\chi}^0_\ell A}, \tag{B10}$$

$$\xi_{RL} = \lambda_{h_i AA} \mathcal{G}^R_{\tilde{\chi}^0_1 \tilde{\chi}^0_\ell A} \mathcal{G}^{R*}_{\tilde{\chi}^0_1 \tilde{\chi}^0_\ell A},$$
$$\xi_{RR} = \lambda_{h_i AA} \mathcal{G}^R_{\tilde{\chi}^0_1 \tilde{\chi}^0_\ell A} \mathcal{G}^{L*}_{\tilde{\chi}^0_1 \tilde{\chi}^0_\ell A}, \tag{B11}$$

where $\lambda_{h_i AA} = -\frac{g_2 M_Z}{2 c_W} c_{2\beta} D_{h_i}$, with $D_{h_i} = \begin{cases} s_{\beta+\alpha}; & h_i = h_1 \\ -c_{\beta+\alpha}; & h_i = h_2 \end{cases}$, $\mathcal{G}^L_{\tilde{\chi}^0_1 \tilde{\chi}^0_\ell A} = i(Q''^*_{\ell 1} s_\beta - S''^*_{\ell 1} c_\beta)$, and $\mathcal{G}^R_{\tilde{\chi}^0_1 \tilde{\chi}^0_\ell A} = i(-Q''_{1\ell} s_\beta + S''_{1\ell} c_\beta)$.

(5) $h_i = h_1/h_2$, $F = \tilde{\chi}^0_\ell$, and $S = A$, $S' = G$ or $S = G$, $S' = A$.

$$\xi_{LL} = \lambda_{h_i AG} \mathcal{G}^L_{\tilde{\chi}^0_1 \tilde{\chi}^0_\ell G} \mathcal{G}^{R*}_{\tilde{\chi}^0_1 \tilde{\chi}^0_\ell A},$$
$$\xi_{LR} = \lambda_{h_i AG} \mathcal{G}^L_{\tilde{\chi}^0_1 \tilde{\chi}^0_\ell G} \mathcal{G}^{L*}_{\tilde{\chi}^0_1 \tilde{\chi}^0_\ell A}, \tag{B12}$$

$$\xi_{RL} = \lambda_{h_i AG} \mathcal{G}^R_{\tilde{\chi}^0_1 \tilde{\chi}^0_\ell G} \mathcal{G}^{R*}_{\tilde{\chi}^0_1 \tilde{\chi}^0_\ell A},$$
$$\xi_{RR} = \lambda_{h_i AG} \mathcal{G}^R_{\tilde{\chi}^0_1 \tilde{\chi}^0_\ell G} \mathcal{G}^{L*}_{\tilde{\chi}^0_1 \tilde{\chi}^0_\ell A}, \tag{B13}$$

where $\lambda_{h_i AG} = -\frac{g_2 M_Z}{2 c_W} s_{2\beta} D_{h_i}$, $\mathcal{G}^L_{\tilde{\chi}^0_1 \tilde{\chi}^0_\ell G} = i g_2 (-Q''^*_{\ell 1} c_\beta - S''^*_{\ell 1} s_\beta)$, and $\mathcal{G}^R_{\tilde{\chi}^0_1 \tilde{\chi}^0_\ell G} = i g_2 (Q''_{1\ell} c_\beta + S''_{1\ell} s_\beta)$.

(6) $h_i = h_1/h_2$, $F = \tilde{\chi}^0_\ell$, and $S = S' = G$.

$$\xi_{LL} = \lambda_{h_i GG} \mathcal{G}^L_{\tilde{\chi}^0_1 \tilde{\chi}^0_\ell G} \mathcal{G}^{R*}_{\tilde{\chi}^0_1 \tilde{\chi}^0_\ell G},$$
$$\xi_{LR} = \lambda_{h_i GG} \mathcal{G}^L_{\tilde{\chi}^0_1 \tilde{\chi}^0_\ell G} \mathcal{G}^{L*}_{\tilde{\chi}^0_1 \tilde{\chi}^0_\ell G}, \tag{B14}$$

$$\xi_{RL} = \lambda_{h_i GG} \mathcal{G}^R_{\tilde{\chi}^0_1 \tilde{\chi}^0_\ell G} \mathcal{G}^{R*}_{\tilde{\chi}^0_1 \tilde{\chi}^0_\ell G},$$
$$\xi_{RR} = \lambda_{h_i GG} \mathcal{G}^R_{\tilde{\chi}^0_1 \tilde{\chi}^0_\ell G} \mathcal{G}^{L*}_{\tilde{\chi}^0_1 \tilde{\chi}^0_\ell G}, \tag{B15}$$

where $\lambda_{h_i GG} = -\frac{g_2 M_Z}{2 c_W} c_{2\beta} D'_{h_i}$, with $D'_{h_i} = \begin{cases} -s_{\beta+\alpha}; & h_i = h_1 \\ c_{\beta+\alpha}; & h_i = h_2 \end{cases}$,

(7) $h_i = h_1/h_2$, $F = \tilde{\chi}^\pm_\ell$, and $S = S' = H^\pm$.

$$\xi_{LL} = \lambda_{h_i H^\pm H^\pm} \mathcal{G}^L_{\tilde{\chi}^0_1 \tilde{\chi}^\pm_\ell H^\pm} \mathcal{G}^{R*}_{\tilde{\chi}^0_1 \tilde{\chi}^\pm_\ell H^\pm},$$
$$\xi_{LR} = \lambda_{h_i H^\pm H^\pm} \mathcal{G}^L_{\tilde{\chi}^0_1 \tilde{\chi}^\pm_\ell H^\pm} \mathcal{G}^{L*}_{\tilde{\chi}^0_1 \tilde{\chi}^\pm_\ell H^\pm}, \tag{B16}$$

$$\xi_{RL} = \lambda_{h_i H^\pm H^\pm} \mathcal{G}^R_{\tilde{\chi}^0_1 \tilde{\chi}^\pm_\ell H^\pm} \mathcal{G}^{R*}_{\tilde{\chi}^0_1 \tilde{\chi}^\pm_\ell H^\pm},$$
$$\xi_{RR} = \lambda_{h_i H^\pm H^\pm} \mathcal{G}^R_{\tilde{\chi}^0_1 \tilde{\chi}^\pm_\ell H^\pm} \mathcal{G}^{L*}_{\tilde{\chi}^0_1 \tilde{\chi}^\pm_\ell H^\pm}, \tag{B17}$$

where, $\lambda_{h_i H^\pm H^\pm} = -g_2 A_{h_i}$, with

$$A_{h_i} = \begin{cases} M_W s_{\beta-\alpha} + \frac{M_Z}{2 c_W} c_{2\beta} s_{\beta+\alpha}; & h_i = h \\ M_W c_{\beta-\alpha} - \frac{M_Z}{2 c_W} c_{2\beta} c_{\beta+\alpha}; & h_i = H \end{cases},$$

$\mathcal{G}^L_{\tilde{\chi}^0_1 \tilde{\chi}^\pm_\ell H^\pm} = -g_2 Q'^L_{1\ell}$, and $\mathcal{G}^R_{\tilde{\chi}^0_1 \tilde{\chi}^\pm_\ell H^\pm} = -g_2 Q'^R_{1\ell}$.

(8) $h_i = h_1/h_2$, $F = \tilde{\chi}^\pm_\ell$, and $S = H^\pm$, $S' = G^\pm$ or $S = G^\pm$, $S' = H^\pm$.

$$\xi_{LL} = \lambda_{h_i H^\pm G^\pm} \mathcal{G}^L_{\tilde{\chi}^0_1 \tilde{\chi}^\pm_\ell G^\pm} \mathcal{G}^{R*}_{\tilde{\chi}^0_1 \tilde{\chi}^\pm_\ell H^\pm},$$
$$\xi_{LR} = \lambda_{h_i H^\pm G^\pm} \mathcal{G}^L_{\tilde{\chi}^0_1 \tilde{\chi}^\pm_\ell G^\pm} \mathcal{G}^{L*}_{\tilde{\chi}^0_1 \tilde{\chi}^\pm_\ell H^\pm}, \tag{B18}$$

$$\xi_{RL} = \lambda_{h_i H^\pm G^\pm} \mathcal{G}^R_{\tilde{\chi}^0_1 \tilde{\chi}^\pm_\ell G^\pm} \mathcal{G}^{R*}_{\tilde{\chi}^0_1 \tilde{\chi}^\pm_\ell H^\pm},$$
$$\xi_{RR} = \lambda_{h_i H^\pm G^\pm} \mathcal{G}^R_{\tilde{\chi}^0_1 \tilde{\chi}^\pm_\ell G^\pm} \mathcal{G}^{L*}_{\tilde{\chi}^0_1 \tilde{\chi}^\pm_\ell H^\pm}, \tag{B19}$$

where $\lambda_{h_i H^\pm G^\pm} = -\frac{g_2 M_W}{2} A'_{h_i}$, with

$$A'_{h_i} = \begin{cases} \frac{s_{2\beta} s_{\beta+\alpha}}{c_W^2} - c_{\beta-\alpha}; & h_i = h_1 \\ -\frac{s_{2\beta} c_{\beta+\alpha}}{c_W^2} - s_{\beta-\alpha}; & h_i = h_2 \end{cases},$$

$\mathcal{G}^L_{\tilde{\chi}^0_1 \tilde{\chi}^\pm_\ell G^\pm} = -g_2 t_\beta Q'^L_{1\ell}$, and $\mathcal{G}^R_{\tilde{\chi}^0_1 \tilde{\chi}^\pm_\ell G^\pm} = \frac{g_2}{t_\beta} Q'^R_{1\ell}$.

(9) $h_i = h_1/h_2$, $F = \tilde{\chi}^\pm_\ell$, and $S = S' = G^\pm$.

$$\xi_{LL} = \lambda_{h_i G^\pm G^\pm} \mathcal{G}^L_{\tilde{\chi}^0_1 \tilde{\chi}^\pm_\ell G^\pm} \mathcal{G}^{R*}_{\tilde{\chi}^0_1 \tilde{\chi}^\pm_\ell G^\pm},$$
$$\xi_{LR} = \lambda_{h_i G^\pm G^\pm} \mathcal{G}^L_{\tilde{\chi}^0_1 \tilde{\chi}^\pm_\ell G^\pm} \mathcal{G}^{L*}_{\tilde{\chi}^0_1 \tilde{\chi}^\pm_\ell G^\pm}, \tag{B20}$$

$$\xi_{RL} = \lambda_{h_i G^\pm G^\pm} \mathcal{G}^R_{\tilde{\chi}^0_1 \tilde{\chi}^\pm_\ell G^\pm} \mathcal{G}^{R*}_{\tilde{\chi}^0_1 \tilde{\chi}^\pm_\ell G^\pm},$$
$$\xi_{RR} = \lambda_{h_i G^\pm G^\pm} \mathcal{G}^R_{\tilde{\chi}^0_1 \tilde{\chi}^\pm_\ell G^\pm} \mathcal{G}^{L*}_{\tilde{\chi}^0_1 \tilde{\chi}^\pm_\ell G^\pm}, \tag{B21}$$

where $\lambda_{h_i G^\pm G^\pm} = -\frac{g_2 M_Z}{2 c_W} c_{2\beta} D'_{h_i}$.

(10) $h_i = h_1/h_2$, $F = q_i$, $S = \tilde{q}_t$, $S' = \tilde{q}_s$

$$\xi_{LL} = \lambda_{h_i \tilde{q}_i \tilde{q}_s} \mathcal{G}^L_{\tilde{\chi}^0_1 q_i \tilde{q}_s} \mathcal{G}^{R*}_{\tilde{\chi}^0_1 q_i \tilde{q}_t},$$
$$\xi_{LR} = \lambda_{h_i \tilde{q}_i \tilde{q}_s} \mathcal{G}^L_{\tilde{\chi}^0_1 q_i \tilde{q}_s} \mathcal{G}^{L*}_{\tilde{\chi}^0_1 q_i \tilde{q}_t}, \tag{B22}$$

$$\xi_{RL} = \lambda_{h_i \tilde{q}_i \tilde{q}_s} \mathcal{G}^R_{\tilde{\chi}^0_1 q_i \tilde{q}_s} \mathcal{G}^{R*}_{\tilde{\chi}^0_1 q_i \tilde{q}_t},$$
$$\xi_{RR} = \lambda_{h_i \tilde{q}_i \tilde{q}_s} \mathcal{G}^R_{\tilde{\chi}^0_1 q_i \tilde{q}_s} \mathcal{G}^{L*}_{\tilde{\chi}^0_1 q_i \tilde{q}_t}, \tag{B23}$$

where $\lambda_{h_i\tilde{q}_t\tilde{q}_s} = C[h_i, \tilde{q}_t, \tilde{q}_s]$ are defined as

$$
\begin{aligned}
C[h_1, \tilde{u}_t, \tilde{u}_s] &= c_A[\tilde{u}_t, \tilde{u}_s]c_\alpha - c_\mu[\tilde{u}_t, \tilde{u}_s]s_\alpha + c_g[\tilde{u}_t, \tilde{u}_s]s_{\alpha+\beta},\\
C[h_1, \tilde{d}_t, \tilde{d}_s] &= -c_A[\tilde{d}_t, \tilde{d}_s]s_\alpha + c_\mu[\tilde{d}_t, \tilde{d}_s]c_\alpha + c_g[\tilde{d}_t, \tilde{d}_s]s_{\alpha+\beta},\\
C[h_2, \tilde{u}_t, \tilde{u}_s] &= c_A[\tilde{u}_t, \tilde{u}_s]s_\alpha + c_\mu[\tilde{u}_t, \tilde{u}_s]c_\alpha - c_g[\tilde{u}_t, \tilde{u}_s]c_{\alpha+\beta},\\
C[h_2, \tilde{d}_t, \tilde{d}_s] &= c_A[\tilde{d}_t, \tilde{d}_s]c_\alpha + c_\mu[\tilde{d}_t, \tilde{d}_s]s_\alpha - c_g[\tilde{d}_t, \tilde{d}_s]c_{\alpha+\beta},
\end{aligned}
$$

with

$$
\begin{aligned}
c_A[\tilde{u}_t,\tilde{u}_s] &= \frac{g_2}{M_W s_\beta}\left\{\frac{1}{2}[W^{\tilde{u}*}_{it}W^{\tilde{u}}_{j+3s}(\mathbf{m_u}A^{u*})_{ij} + W^{\tilde{u}*}_{j+3t}W^{\tilde{u}}_{is}(\mathbf{m_u}^*A^u)_{ij}]\right\} - m^2_{u_k}[U^{u_L}_{ik}U^{u_L*}_{jk}W^{\tilde{u}*}_{it}W^{\tilde{u}}_{js} + U^{u_R}_{ik}U^{u_R*}_{jk}W^{\tilde{u}*}_{i+3t}W^{\tilde{u}}_{j+3s}],\\
c_A[\tilde{d}_t,\tilde{d}_s] &= \frac{g_2}{M_W c_\beta}\left\{\frac{1}{2}[W^{\tilde{d}*}_{it}W^{\tilde{d}}_{j+3s}(\mathbf{m_d}A^{d*})_{ij} + W^{\tilde{d}*}_{j+3t}W^{\tilde{d}}_{is}(\mathbf{m_d}^*A^d)_{ij}]\right\} - m^2_{d_k}[U^{d_L}_{ik}U^{d_L*}_{jk}W^{\tilde{d}*}_{it}W^{\tilde{d}}_{js} + U^{d_R}_{ik}U^{d_R*}_{jk}W^{\tilde{d}*}_{i+3t}W^{\tilde{d}}_{j+3s}],\\
c_\mu[\tilde{u}_t,\tilde{u}_s] &= \frac{g_2}{2M_W s_\beta}m_{u_k}[\mu U^{u_L}_{ik}U^{u_R*}_{jk}W^{\tilde{u}*}_{it}W^{\tilde{u}}_{j+3s} + \mu^* U^{u_L*}_{ik}U^{u_R}_{jk}W^{\tilde{u}*}_{j+3t}W^{\tilde{u}}_{is}],\\
c_\mu[\tilde{d}_t,\tilde{d}_s] &= \frac{g_2}{2M_W c_\beta}m_{d_k}[\mu U^{d_L}_{ik}U^{d_R*}_{jk}W^{\tilde{d}*}_{it}W^{\tilde{d}}_{j+3s} + \mu^* U^{d_L*}_{ik}U^{d_R}_{jk}W^{\tilde{d}*}_{j+3t}W^{\tilde{d}}_{is}],\\
c_g[\tilde{u}_t,\tilde{u}_s] &= \frac{g_2 M_W}{2}\left[W^{\tilde{u}*}_{it}W^{\tilde{u}}_{is}\left(1-\frac{1}{3}t^2_W\right) + \frac{4}{3}W^{\tilde{u}*}_{i+3t}W^{\tilde{u}}_{i+3s}t^2_W\right],\\
c_g[\tilde{d}_t,\tilde{d}_s] &= -\frac{g_2 M_W}{2}\left[W^{\tilde{d}*}_{it}W^{\tilde{d}}_{is}\left(1+\frac{1}{3}t^2_W\right) + \frac{2}{3}W^{\tilde{d}*}_{i+3t}W^{\tilde{d}}_{i+3s}t^2_W\right].
\end{aligned}
$$

In the present context, only the third-generation quarks and squarks have been included, and no flavor mixing in the squark sector has been assumed. Further, the third-generation squarks are kept lighter than the first two generations. Thus, in the subscripts only $t, s \in \{1, 2\}$ are relevant; further $i, j, k = 3$. The same treatment follows for all the subsequent diagrams, including the third-generation (s)quark loops.

2. Topology-(1b)

The respective Feynman diagram is shown in Fig. 5(b).

$$
\begin{aligned}
i\delta\Gamma^{(b)} = -\frac{i}{16\pi^2}[&P_L\{\zeta_{LRL}\mathbf{B}_0 + \zeta_{LLL}m_F m_{F'}\mathbf{C}_0 + \zeta_{LLR}m_{\tilde{\chi}^0_1}m_{F'}(\mathbf{C}_0 + \mathbf{C}_1) + \zeta_{LRL}m^2_S\mathbf{C}_0\\
&+ \zeta_{LRL}m^2_{\tilde{\chi}^0_1}(2\mathbf{C}_0 + 3\mathbf{C}_1 + 3\mathbf{C}_2) - \zeta_{LRL}q^2(\mathbf{C}_0 + \mathbf{C}_1 + \mathbf{C}_2) - \zeta_{LRL}(2m^2_{\tilde{\chi}^0_1} - q^2).\\
&(\mathbf{C}_0 + \mathbf{C}_1 + \mathbf{C}_2) + \zeta_{LRR}m_{\tilde{\chi}^0_1}m_F\mathbf{C}_1 + \zeta_{RLL}m_{\tilde{\chi}^0_1}m_F(\mathbf{C}_0 + \mathbf{C}_2)\\
&+ \zeta_{RLR}m^2_{\tilde{\chi}^0_1}(\mathbf{C}_0 + \mathbf{C}_1 + \mathbf{C}_2) + \zeta_{RRL}m_{\tilde{\chi}^0_1}m_{F'}\mathbf{C}_2\}\\
&+ P_R\{\zeta_{RLR}\mathbf{B}_0 + \zeta_{LLR}m_{\tilde{\chi}^0_1}m_{F'}\mathbf{C}_2 + \zeta_{LRL}m^2_{\tilde{\chi}^0_1}(\mathbf{C}_0 + \mathbf{C}_1 + \mathbf{C}_2) + \zeta_{LRR}m_{\tilde{\chi}^0_1}m_F(\mathbf{C}_0\\
&+ \mathbf{C}_2) + \zeta_{RLL}m_{\tilde{\chi}^0_1}m_F\mathbf{C}_1 + \zeta_{RLR}m^2_S\mathbf{C}_0 + \zeta_{RLR}m^2_{\tilde{\chi}^0_1}(2\mathbf{C}_0 + 3\mathbf{C}_1 + 3\mathbf{C}_2) - \zeta_{RLR}q^2.\\
&(\mathbf{C}_0 + \mathbf{C}_1 + \mathbf{C}_2) - \zeta_{RLR}(2m^2_{\tilde{\chi}^0_1} - q^2)(\mathbf{C}_0 + \mathbf{C}_1 + \mathbf{C}_2) + \zeta_{RRL}m_{\tilde{\chi}^0_1}m_{F'}(\mathbf{C}_0 + \mathbf{C}_1) + \zeta_{RRR}m_F m_{F'}\mathbf{C}_0\}],
\end{aligned}
\tag{B24}
$$

where $\mathbf{B}_0 = \mathbf{B}_0(q^2; m_F, m_{F'})$, $\mathbf{C}_i = \mathbf{C}_i(m^2_{\tilde{\chi}^0_1}, q^2, m^2_{\tilde{\chi}^0_1}; m_S, m_F, m_{F'})$ and

$$
\begin{aligned}
\zeta_{LLL} &= \mathscr{G}^L_{\tilde{\chi}^0_1F'S}\mathscr{G}^L_{FF'h_i}\mathscr{G}^L_{\tilde{\chi}^0_1FS},\\
\zeta_{LLR} &= \mathscr{G}^L_{\tilde{\chi}^0_1F'S}\mathscr{G}^L_{FF'h_i}\mathscr{G}^R_{\tilde{\chi}^0_1FS},
\end{aligned}
\tag{B25}
$$

$$
\begin{aligned}
\zeta_{LRL} &= \mathscr{G}^L_{\tilde{\chi}^0_1F'S}\mathscr{G}^R_{FF'h_i}\mathscr{G}^L_{\tilde{\chi}^0_1FS},\\
\zeta_{LRR} &= \mathscr{G}^L_{\tilde{\chi}^0_1F'S}\mathscr{G}^R_{FF'h_i}\mathscr{G}^R_{\tilde{\chi}^0_1FS},
\end{aligned}
\tag{B26}
$$

$$
\begin{aligned}
\zeta_{RLL} &= \mathscr{G}^R_{\tilde{\chi}^0_1F'S}\mathscr{G}^L_{FF'h_i}\mathscr{G}^L_{\tilde{\chi}^0_1FS},\\
\zeta_{RLR} &= \mathscr{G}^R_{\tilde{\chi}^0_1F'S}\mathscr{G}^L_{FF'h_i}\mathscr{G}^R_{\tilde{\chi}^0_1FS},
\end{aligned}
\tag{B27}
$$

$$\zeta_{RRL} = \mathcal{G}^R_{\tilde{\chi}^0_1 F' S}\mathcal{G}^R_{FF'h_i}\mathcal{G}^L_{\tilde{\chi}^0_1 FS},$$
$$\zeta_{RRR} = \mathcal{G}^R_{\tilde{\chi}^0_1 F' S}\mathcal{G}^R_{FF'h_i}\mathcal{G}^R_{\tilde{\chi}^0_1 FS}. \tag{B28}$$

(1) $h_i = h_1/h_2$, $S = h_1/h_2$, $F = \tilde{\chi}^0_\ell$, $F' = \tilde{\chi}^0_n$.

$$\zeta_{LLL} = \mathcal{G}^L_{\tilde{\chi}^0_1\tilde{\chi}^0_n h_i}\mathcal{G}^L_{\tilde{\chi}^0_\ell\tilde{\chi}^0_n h_i}\mathcal{G}^{R*}_{\tilde{\chi}^0_1\tilde{\chi}^0_\ell h_i},$$
$$\zeta_{LLR} = \mathcal{G}^L_{\tilde{\chi}^0_1\tilde{\chi}^0_n h_i}\mathcal{G}^L_{\tilde{\chi}^0_\ell\tilde{\chi}^0_n h_i}\mathcal{G}^{L*}_{\tilde{\chi}^0_1\tilde{\chi}^0_\ell h_i}, \tag{B29}$$

$$\zeta_{LRL} = \mathcal{G}^L_{\tilde{\chi}^0_1\tilde{\chi}^0_n h_i}\mathcal{G}^R_{\tilde{\chi}^0_\ell\tilde{\chi}^0_n h_i}\mathcal{G}^{R*}_{\tilde{\chi}^0_1\tilde{\chi}^0_\ell h_i},$$
$$\zeta_{LRR} = \mathcal{G}^L_{\tilde{\chi}^0_1\tilde{\chi}^0_n h_i}\mathcal{G}^R_{\tilde{\chi}^0_\ell\tilde{\chi}^0_n h_i}\mathcal{G}^{L*}_{\tilde{\chi}^0_1\tilde{\chi}^0_\ell h_i}, \tag{B30}$$

$$\zeta_{RLL} = \mathcal{G}^R_{\tilde{\chi}^0_1\tilde{\chi}^0_n h_i}\mathcal{G}^L_{\tilde{\chi}^0_\ell\tilde{\chi}^0_n h_i}\mathcal{G}^{R*}_{\tilde{\chi}^0_1\tilde{\chi}^0_\ell h_i},$$
$$\zeta_{RLR} = \mathcal{G}^R_{\tilde{\chi}^0_1\tilde{\chi}^0_n h_i}\mathcal{G}^L_{\tilde{\chi}^0_\ell\tilde{\chi}^0_n h_i}\mathcal{G}^{L*}_{\tilde{\chi}^0_1\tilde{\chi}^0_\ell h_i}, \tag{B31}$$

$$\zeta_{RRL} = \mathcal{G}^R_{\tilde{\chi}^0_1\tilde{\chi}^0_n h_i}\mathcal{G}^R_{\tilde{\chi}^0_\ell\tilde{\chi}^0_n h_i}\mathcal{G}^{R*}_{\tilde{\chi}^0_1\tilde{\chi}^0_\ell h_i},$$
$$\zeta_{RRR} = \mathcal{G}^R_{\tilde{\chi}^0_1\tilde{\chi}^0_n h_i}\mathcal{G}^R_{\tilde{\chi}^0_\ell\tilde{\chi}^0_n h_i}\mathcal{G}^{L*}_{\tilde{\chi}^0_1\tilde{\chi}^0_\ell h_i}, \tag{B32}$$

where

$$\mathcal{G}^L_{\tilde{\chi}^0_\ell\tilde{\chi}^0_n h_i} = \begin{cases} g_2(Q''^*_{\ell n}s_\alpha + S''^*_{\ell n}c_\alpha); & h_i = h_1 \\ -g_2(Q''^*_{\ell n}c_\alpha - S''^*_{\ell n}s_\alpha); & h_i = h_2 \end{cases},$$

and

$$\mathcal{G}^R_{\tilde{\chi}^0_\ell\tilde{\chi}^0_n h_i} = \begin{cases} g_2(Q''_{n\ell}s_\alpha + S''_{n\ell}c_\alpha); & h_i = h_1 \\ -g_2(Q''_{n\ell}c_\alpha - S''_{n\ell}s_\alpha); & h_i = h_2 \end{cases}.$$

(2) $h_i = h_1/h_2$, $S = A$, $F = \tilde{\chi}^0_\ell$, $F' = \tilde{\chi}^0_n$.

$$\zeta_{LLL} = \mathcal{G}^L_{\tilde{\chi}^0_1\tilde{\chi}^0_n A}\mathcal{G}^L_{\tilde{\chi}^0_\ell\tilde{\chi}^0_n h_i}\mathcal{G}^{R*}_{\tilde{\chi}^0_1\tilde{\chi}^0_\ell A},$$
$$\zeta_{LLR} = \mathcal{G}^L_{\tilde{\chi}^0_1\tilde{\chi}^0_n A}\mathcal{G}^L_{\tilde{\chi}^0_\ell\tilde{\chi}^0_n h_i}\mathcal{G}^{L*}_{\tilde{\chi}^0_1\tilde{\chi}^0_\ell A}, \tag{B33}$$

$$\zeta_{LRL} = \mathcal{G}^L_{\tilde{\chi}^0_1\tilde{\chi}^0_n A}\mathcal{G}^R_{\tilde{\chi}^0_\ell\tilde{\chi}^0_n h_i}\mathcal{G}^{R*}_{\tilde{\chi}^0_1\tilde{\chi}^0_\ell A},$$
$$\zeta_{LRR} = \mathcal{G}^L_{\tilde{\chi}^0_1\tilde{\chi}^0_n A}\mathcal{G}^R_{\tilde{\chi}^0_\ell\tilde{\chi}^0_n h_i}\mathcal{G}^{L*}_{\tilde{\chi}^0_1\tilde{\chi}^0_\ell A}, \tag{B34}$$

$$\zeta_{RLL} = \mathcal{G}^R_{\tilde{\chi}^0_1\tilde{\chi}^0_n A}\mathcal{G}^L_{\tilde{\chi}^0_\ell\tilde{\chi}^0_n h_i}\mathcal{G}^{R*}_{\tilde{\chi}^0_1\tilde{\chi}^0_\ell A},$$
$$\zeta_{RLR} = \mathcal{G}^R_{\tilde{\chi}^0_1\tilde{\chi}^0_n A}\mathcal{G}^L_{\tilde{\chi}^0_\ell\tilde{\chi}^0_n h_i}\mathcal{G}^{L*}_{\tilde{\chi}^0_1\tilde{\chi}^0_\ell A}, \tag{B35}$$

$$\zeta_{RRL} = \mathcal{G}^R_{\tilde{\chi}^0_1\tilde{\chi}^0_n A}\mathcal{G}^R_{\tilde{\chi}^0_\ell\tilde{\chi}^0_n h_i}\mathcal{G}^{R*}_{\tilde{\chi}^0_1\tilde{\chi}^0_\ell A},$$
$$\zeta_{RRR} = \mathcal{G}^R_{\tilde{\chi}^0_1\tilde{\chi}^0_n A}\mathcal{G}^R_{\tilde{\chi}^0_\ell\tilde{\chi}^0_n h_i}\mathcal{G}^{L*}_{\tilde{\chi}^0_1\tilde{\chi}^0_\ell A}, \tag{B36}$$

where $\mathcal{G}^L_{\tilde{\chi}^0_1\tilde{\chi}^0_n A} = i(Q''^*_{n1}s_\beta - S''^*_{n1}c_\beta)$ and $\mathcal{G}^R_{\tilde{\chi}^0_1\tilde{\chi}^0_n A} = i(-Q''_{1n}s_\beta + S''_{1n}c_\beta)$.

(3) $h_i = h_1/h_2$, $S = G$, $F = \tilde{\chi}^0_\ell$, $F' = \tilde{\chi}^0_n$.

$$\zeta_{LLL} = \mathcal{G}^L_{\tilde{\chi}^0_1\tilde{\chi}^0_n G}\mathcal{G}^L_{\tilde{\chi}^0_\ell\tilde{\chi}^0_n h_i}\mathcal{G}^{R*}_{\tilde{\chi}^0_1\tilde{\chi}^0_\ell G},$$
$$\zeta_{LLR} = \mathcal{G}^L_{\tilde{\chi}^0_1\tilde{\chi}^0_n G}\mathcal{G}^L_{\tilde{\chi}^0_\ell\tilde{\chi}^0_n h_i}\mathcal{G}^{L*}_{\tilde{\chi}^0_1\tilde{\chi}^0_\ell G}, \tag{B37}$$

$$\zeta_{LRL} = \mathcal{G}^L_{\tilde{\chi}^0_1\tilde{\chi}^0_n G}\mathcal{G}^R_{\tilde{\chi}^0_\ell\tilde{\chi}^0_n h_i}\mathcal{G}^{R*}_{\tilde{\chi}^0_1\tilde{\chi}^0_\ell G},$$
$$\zeta_{LRR} = \mathcal{G}^L_{\tilde{\chi}^0_1\tilde{\chi}^0_n G}\mathcal{G}^R_{\tilde{\chi}^0_\ell\tilde{\chi}^0_n h_i}\mathcal{G}^{L*}_{\tilde{\chi}^0_1\tilde{\chi}^0_\ell G}, \tag{B38}$$

$$\zeta_{RLL} = \mathcal{G}^R_{\tilde{\chi}^0_1\tilde{\chi}^0_n G}\mathcal{G}^L_{\tilde{\chi}^0_\ell\tilde{\chi}^0_n h_i}\mathcal{G}^{R*}_{\tilde{\chi}^0_1\tilde{\chi}^0_\ell G},$$
$$\zeta_{RLR} = \mathcal{G}^R_{\tilde{\chi}^0_1\tilde{\chi}^0_n G}\mathcal{G}^L_{\tilde{\chi}^0_\ell\tilde{\chi}^0_n h_i}\mathcal{G}^{L*}_{\tilde{\chi}^0_1\tilde{\chi}^0_\ell G}, \tag{B39}$$

$$\zeta_{RRL} = \mathcal{G}^R_{\tilde{\chi}^0_1\tilde{\chi}^0_n G}\mathcal{G}^R_{\tilde{\chi}^0_\ell\tilde{\chi}^0_n h_i}\mathcal{G}^{R*}_{\tilde{\chi}^0_1\tilde{\chi}^0_\ell G},$$
$$\zeta_{RRR} = \mathcal{G}^R_{\tilde{\chi}^0_1\tilde{\chi}^0_n G}\mathcal{G}^R_{\tilde{\chi}^0_\ell\tilde{\chi}^0_n h_i}\mathcal{G}^{L*}_{\tilde{\chi}^0_1\tilde{\chi}^0_\ell G}. \tag{B40}$$

(4) $h_i = h_1/h_2$, $S = H^\pm$, $F = \tilde{\chi}^\pm_\ell$, $F' = \tilde{\chi}^\pm_n$.

$$\zeta_{LLL} = \mathcal{G}^L_{\tilde{\chi}^0_1\tilde{\chi}^\pm_n H^\pm}\mathcal{G}^L_{\tilde{\chi}^\pm_\ell\tilde{\chi}^\pm_n h_i}\mathcal{G}^{R*}_{\tilde{\chi}^0_1\tilde{\chi}^\pm_\ell H^\pm},$$
$$\zeta_{LLR} = \mathcal{G}^L_{\tilde{\chi}^0_1\tilde{\chi}^\pm_n H^\pm}\mathcal{G}^L_{\tilde{\chi}^\pm_\ell\tilde{\chi}^\pm_n h_i}\mathcal{G}^{L*}_{\tilde{\chi}^0_1\tilde{\chi}^\pm_\ell H^\pm}, \tag{B41}$$

$$\zeta_{LRL} = \mathcal{G}^L_{\tilde{\chi}^0_1\tilde{\chi}^\pm_n H^\pm}\mathcal{G}^R_{\tilde{\chi}^\pm_\ell\tilde{\chi}^\pm_n h_i}\mathcal{G}^{R*}_{\tilde{\chi}^0_1\tilde{\chi}^\pm_\ell H^\pm},$$
$$\zeta_{LRR} = \mathcal{G}^L_{\tilde{\chi}^0_1\tilde{\chi}^\pm_n H^\pm}\mathcal{G}^R_{\tilde{\chi}^\pm_\ell\tilde{\chi}^\pm_n h_i}\mathcal{G}^{L*}_{\tilde{\chi}^0_1\tilde{\chi}^\pm_\ell H^\pm}, \tag{B42}$$

$$\zeta_{RLL} = \mathcal{G}^R_{\tilde{\chi}^0_1\tilde{\chi}^\pm_n H^\pm}\mathcal{G}^L_{\tilde{\chi}^\pm_\ell\tilde{\chi}^\pm_n h_i}\mathcal{G}^{R*}_{\tilde{\chi}^0_1\tilde{\chi}^\pm_\ell H^\pm},$$
$$\zeta_{RLR} = \mathcal{G}^R_{\tilde{\chi}^0_1\tilde{\chi}^\pm_n H^\pm}\mathcal{G}^L_{\tilde{\chi}^\pm_\ell\tilde{\chi}^\pm_n h_i}\mathcal{G}^{L*}_{\tilde{\chi}^0_1\tilde{\chi}^\pm_\ell H^\pm}, \tag{B43}$$

$$\zeta_{RRL} = \mathcal{G}^R_{\tilde{\chi}^0_1\tilde{\chi}^\pm_n H^\pm}\mathcal{G}^R_{\tilde{\chi}^\pm_\ell\tilde{\chi}^\pm_n h_i}\mathcal{G}^{R*}_{\tilde{\chi}^0_1\tilde{\chi}^\pm_\ell H^\pm},$$
$$\zeta_{RRR} = \mathcal{G}^R_{\tilde{\chi}^0_1\tilde{\chi}^\pm_n H^\pm}\mathcal{G}^R_{\tilde{\chi}^\pm_\ell\tilde{\chi}^\pm_n h_i}\mathcal{G}^{L*}_{\tilde{\chi}^0_1\tilde{\chi}^\pm_\ell H^\pm}. \tag{B44}$$

(5) $h_i = h_1/h_2$, $S = G^\pm$, $F = \tilde{\chi}^\pm_\ell$, $F' = \tilde{\chi}^\pm_n$.

$$\zeta_{LLL} = \mathcal{G}^L_{\tilde{\chi}^0_1\tilde{\chi}^\pm_n G^\pm}\mathcal{G}^L_{\tilde{\chi}^\pm_\ell\tilde{\chi}^\pm_n h_i}\mathcal{G}^{R*}_{\tilde{\chi}^0_1\tilde{\chi}^\pm_\ell G^\pm},$$
$$\zeta_{LLR} = \mathcal{G}^L_{\tilde{\chi}^0_1\tilde{\chi}^\pm_n G^\pm}\mathcal{G}^L_{\tilde{\chi}^\pm_\ell\tilde{\chi}^\pm_n h_i}\mathcal{G}^{L*}_{\tilde{\chi}^0_1\tilde{\chi}^\pm_\ell G^\pm}, \tag{B45}$$

$$\zeta_{LRL} = \mathcal{G}^L_{\tilde{\chi}^0_1\tilde{\chi}^\pm_n G^\pm}\mathcal{G}^R_{\tilde{\chi}^\pm_\ell\tilde{\chi}^\pm_n h_i}\mathcal{G}^{R*}_{\tilde{\chi}^0_1\tilde{\chi}^\pm_\ell G^\pm},$$
$$\zeta_{LRR} = \mathcal{G}^L_{\tilde{\chi}^0_1\tilde{\chi}^\pm_n G^\pm}\mathcal{G}^R_{\tilde{\chi}^\pm_\ell\tilde{\chi}^\pm_n h_i}\mathcal{G}^{L*}_{\tilde{\chi}^0_1\tilde{\chi}^\pm_\ell G^\pm}, \tag{B46}$$

$$\zeta_{RLL} = \mathcal{G}^R_{\tilde{\chi}^0_1\tilde{\chi}^\pm_n G^\pm}\mathcal{G}^L_{\tilde{\chi}^\pm_\ell\tilde{\chi}^\pm_n h_i}\mathcal{G}^{R*}_{\tilde{\chi}^0_1\tilde{\chi}^\pm_\ell G^\pm},$$
$$\zeta_{RLR} = \mathcal{G}^R_{\tilde{\chi}^0_1\tilde{\chi}^\pm_n G^\pm}\mathcal{G}^L_{\tilde{\chi}^\pm_\ell\tilde{\chi}^\pm_n h_i}\mathcal{G}^{L*}_{\tilde{\chi}^0_1\tilde{\chi}^\pm_\ell G^\pm}, \tag{B47}$$

$$\zeta_{RRL} = \mathcal{G}^R_{\tilde{\chi}^0_1\tilde{\chi}^\pm_n G^\pm}\mathcal{G}^R_{\tilde{\chi}^\pm_\ell\tilde{\chi}^\pm_n h_i}\mathcal{G}^{R*}_{\tilde{\chi}^0_1\tilde{\chi}^\pm_\ell G^\pm},$$
$$\zeta_{RRR} = \mathcal{G}^R_{\tilde{\chi}^0_1\tilde{\chi}^\pm_n G^\pm}\mathcal{G}^R_{\tilde{\chi}^\pm_\ell\tilde{\chi}^\pm_n h_i}\mathcal{G}^{L*}_{\tilde{\chi}^0_1\tilde{\chi}^\pm_\ell G^\pm}. \tag{B48}$$

(6) $h_i = h_1/h_2$, $F = F' = q_i$, $S = \tilde{q}_s$.

$$\zeta_{LLL} = \mathcal{G}^{L}_{\tilde{\chi}^0_1 q_i \tilde{q}_s} \mathcal{G}^{L}_{q_i q_i h_i} \mathcal{G}^{R*}_{\tilde{\chi}^0_1 q_i \tilde{q}_s},$$
$$\zeta_{LLR} = \mathcal{G}^{L}_{\tilde{\chi}^0_1 q_i \tilde{q}_s} \mathcal{G}^{L}_{q_i q_i h_i} \mathcal{G}^{L*}_{\tilde{\chi}^0_1 q_i \tilde{q}_s}, \tag{B49}$$

$$\zeta_{LRL} = \mathcal{G}^{L}_{\tilde{\chi}^0_1 q_i \tilde{q}_s} \mathcal{G}^{R}_{q_i q_i h_i} \mathcal{G}^{R*}_{\tilde{\chi}^0_1 q_i \tilde{q}_s},$$
$$\zeta_{LRR} = \mathcal{G}^{L}_{\tilde{\chi}^0_1 q_i \tilde{q}_s} \mathcal{G}^{R}_{q_i q_i h_i} \mathcal{G}^{L*}_{\tilde{\chi}^0_1 q_i \tilde{q}_s}, \tag{B50}$$

$$\zeta_{RLL} = \mathcal{G}^{R}_{\tilde{\chi}^0_1 q_i \tilde{q}_s} \mathcal{G}^{L}_{q_i q_i h_i} \mathcal{G}^{R*}_{\tilde{\chi}^0_1 q_i \tilde{q}_s},$$
$$\zeta_{RLR} = \mathcal{G}^{R}_{\tilde{\chi}^0_1 q_i \tilde{q}_s} \mathcal{G}^{L}_{q_i q_i h_i} \mathcal{G}^{L*}_{\tilde{\chi}^0_1 q_i \tilde{q}_s}, \tag{B51}$$

$$\zeta_{RRL} = \mathcal{G}^{R}_{\tilde{\chi}^0_1 q_i \tilde{q}_s} \mathcal{G}^{R}_{q_i q_i h_i} \mathcal{G}^{R*}_{\tilde{\chi}^0_1 q_i \tilde{q}_s},$$
$$\zeta_{RRR} = \mathcal{G}^{R}_{\tilde{\chi}^0_1 q_i \tilde{q}_s} \mathcal{G}^{R}_{q_i q_i h_i} \mathcal{G}^{L*}_{\tilde{\chi}^0_1 q_i \tilde{q}_s}, \tag{B52}$$

where $\mathcal{G}^{L}_{q_i q_i h_i} = \mathcal{G}^{R}_{q_i q_i h_i} = -g_2 \frac{m_{q_i}}{2M_W} \mathcal{X}_{q_i q_i h_i}$, $\mathcal{G}^{L}_{\tilde{\chi}^0_1 q_i \tilde{q}_s} = G^{q_L}_{is1}$ and $\mathcal{G}^{R}_{\tilde{\chi}^0_1 q_i \tilde{q}_s} = G^{q_R}_{is1}$; $q = u, d$; $i = 3$; $s = 1, 2$; with $\mathcal{X}_{u_i u_i h_i} = \begin{cases} \frac{c_\alpha}{s_\beta}; & h_i = h_1 \\ \frac{s_\alpha}{s_\beta}; & h_i = h_2 \end{cases}$, $\mathcal{X}_{d_i d_i h_i} = \begin{cases} \frac{-s_\alpha}{c_\beta}; & h_i = h_1 \\ \frac{c_\alpha}{c_\beta}; & h_i = h_2 \end{cases}$,

$$\mathrm{G}^{u_L}_{is1} = -\sqrt{2} g_2 \left(\frac{1}{2} N^*_{12} + \frac{1}{6} \tan\theta_W N^*_{11} \right) W^{\tilde{u}*}_{js} U^{u_L}_{ji} - \frac{g_2}{\sqrt{2} M_W \sin\beta} m_{u_i} N^*_{14} W^{\tilde{u}*}_{j+3} U^{u_R}_{ji},$$
$$\mathrm{G}^{u_R}_{is1} = \frac{2\sqrt{2}}{3} g_2 \tan\theta_W N_{11} W^{\tilde{u}*}_{j+3} U^{u_R}_{ji} - \frac{g_2}{\sqrt{2} M_W \sin\beta} m_{u_i} N_{14} W^{\tilde{u}*}_{js} U^{u_L}_{ji},$$
$$\mathrm{G}^{d_L}_{is1} = \sqrt{2} g_2 \left(\frac{1}{2} N^*_{12} - \frac{1}{6} \tan\theta_W N^*_{11} \right) W^{\tilde{d}*}_{js} U^{d_L}_{ji} - \frac{g_2}{\sqrt{2} M_W \cos\beta} m_{d_i} N^*_{13} W^{\tilde{d}*}_{j+3} U^{d_R}_{ji},$$
$$\mathrm{G}^{d_R}_{is1} = -\frac{\sqrt{2}}{3} g_2 \tan\theta_W N_{11} W^{\tilde{d}*}_{j+3} U^{d_R}_{ji} - \frac{g_2}{\sqrt{2} M_W \cos\beta} m_{d_i} N_{13} W^{\tilde{d}*}_{js} U^{d_L}_{ji}.$$

For third-generation quarks and squarks: $i, j = 3$ and $s \in \{1, 2\}$.

3. Topology-(2a)

The respective Feynman diagram is shown in Fig. 6(a).

$$\begin{aligned} i\delta\Gamma^{(c)} = \frac{i}{16\pi^2} [& P_L \{ \Lambda_{LLL} m_{\tilde{\chi}^0_1} m_{F'} (2-d) \mathbf{C}_2 + \Lambda_{LRL} m_{\tilde{\chi}^0_1} m_F (2-d)(\mathbf{C}_0 + \mathbf{C}_2) + \Lambda_{LRR} m^2_{\tilde{\chi}^0_1} (d-4)(\mathbf{C}_0 + \mathbf{C}_1 + \mathbf{C}_2) \\ & + \Lambda_{RLL} \{ d\mathbf{B}_0 + (4m^2_{\tilde{\chi}^0_1} + m^2_V d - 2q^2)\mathbf{C}_0 + (4m^2_{\tilde{\chi}^0_1} + m^2_{\tilde{\chi}^0_1} d - 2q^2)(\mathbf{C}_1 + \mathbf{C}_2) \} \\ & + \Lambda_{RLR} m_{\tilde{\chi}^0_1} m_F (2-d)\mathbf{C}_1 + \Lambda_{RRL} m_F m_{F'} d\mathbf{C}_0 + \Lambda_{RRR} m_{\tilde{\chi}^0_1} m_{F'} (2-d)(\mathbf{C}_0 + \mathbf{C}_1) \} \\ & + P_R \{ \Lambda_{LLL} m_{\tilde{\chi}^0_1} m_{F'} (\mathbf{C}_0 + \mathbf{C}_1) + \Lambda_{LLR} m_F m_{F'} d\mathbf{C}_0 + \Lambda_{LRL} m_{\tilde{\chi}^0_1} m_F (2-d)\mathbf{C}_1 \\ & + \Lambda_{LRR} \{ d\mathbf{B}_0 + (4m^2_{\tilde{\chi}^0_1} + m^2_V d - 2q^2)\mathbf{C}_0 + (4m^2_{\tilde{\chi}^0_1} + m^2_{\tilde{\chi}^0_1} d - 2q^2)(\mathbf{C}_1 + \mathbf{C}_2) \} \\ & + \Lambda_{RLL} m^2_{\tilde{\chi}^0_1} (d-4)(\mathbf{C}_0 + \mathbf{C}_1 + \mathbf{C}_2) + \Lambda_{RLR} m_{\tilde{\chi}^0_1} m_F (2-d)(\mathbf{C}_0 + \mathbf{C}_2) + \Lambda_{RRR} m_{\tilde{\chi}^0_1} m_{F'} (2-d)\mathbf{C}_2 \}], \end{aligned} \tag{B53}$$

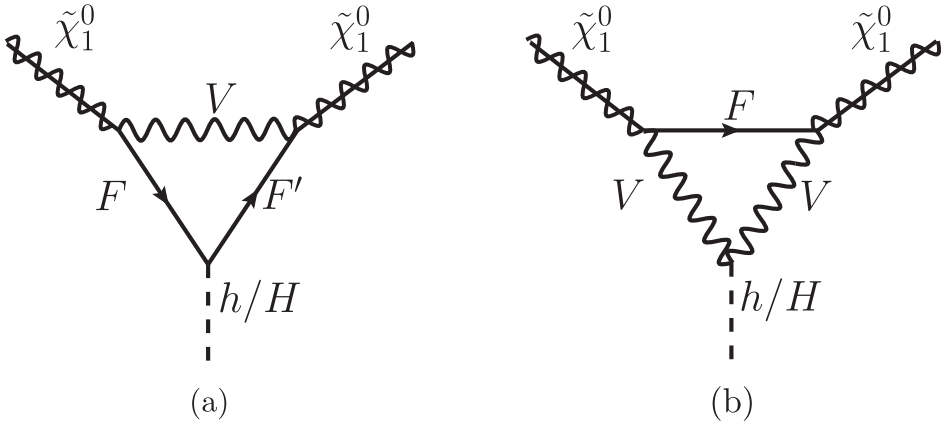

FIG. 6. Topology 2(a) and 2(b).

where $\mathbf{B}_0 = \mathbf{B}_0(q^2, m_F, m_{F'})$, $\mathbf{C}_i = \mathbf{C}_i(m^2_{\tilde{\chi}^0_1}, q^2, m^2_{\tilde{\chi}^0_1}; m_V, m_F, m_{F'})$ and

$$\Lambda_{LLL} = \mathcal{G}^L_{\tilde{\chi}^0_1 F' V}\mathcal{G}^L_{FF' h_i}\mathcal{G}^L_{\tilde{\chi}^0_1 FV},$$
$$\Lambda_{LLR} = \mathcal{G}^L_{\tilde{\chi}^0_1 F' V}\mathcal{G}^L_{FF' h_i}\mathcal{G}^R_{\tilde{\chi}^0_1 FV}, \tag{B54}$$

$$\Lambda_{LRL} = \mathcal{G}^L_{\tilde{\chi}^0_1 F' V}\mathcal{G}^R_{FF' h_i}\mathcal{G}^L_{\tilde{\chi}^0_1 FV},$$
$$\Lambda_{LRR} = \mathcal{G}^L_{\tilde{\chi}^0_1 F' V}\mathcal{G}^R_{FF' h_i}\mathcal{G}^R_{\tilde{\chi}^0_1 FV}, \tag{B55}$$

$$\Lambda_{RLL} = \mathcal{G}^R_{\tilde{\chi}^0_1 F' V}\mathcal{G}^L_{FF' h_i}\mathcal{G}^L_{\tilde{\chi}^0_1 FV},$$
$$\Lambda_{RLR} = \mathcal{G}^R_{\tilde{\chi}^0_1 F' V}\mathcal{G}^L_{FF' h_i}\mathcal{G}^R_{\tilde{\chi}^0_1 FV}, \tag{B56}$$

$$\Lambda_{RRL} = \mathcal{G}^R_{\tilde{\chi}^0_1 F' V}\mathcal{G}^R_{FF' h_i}\mathcal{G}^L_{\tilde{\chi}^0_1 FV},$$
$$\Lambda_{RRR} = \mathcal{G}^R_{\tilde{\chi}^0_1 F' V}\mathcal{G}^R_{FF' h_i}\mathcal{G}^R_{\tilde{\chi}^0_1 FV}. \tag{B57}$$

(1) $h_i = h_1/h_2$, $F = \tilde{\chi}^0_\ell$, $F' = \tilde{\chi}^0_n$, $V = Z$.

$$\Lambda_{LLL} = \mathcal{G}^L_{\tilde{\chi}^0_1\tilde{\chi}^0_n Z}\mathcal{G}^L_{\tilde{\chi}^0_\ell\tilde{\chi}^0_n h_i}\mathcal{G}^{L*}_{\tilde{\chi}^0_1\tilde{\chi}^0_\ell Z},$$
$$\Lambda_{LLR} = -\mathcal{G}^L_{\tilde{\chi}^0_1\tilde{\chi}^0_n Z}\mathcal{G}^L_{\tilde{\chi}^0_\ell\tilde{\chi}^0_n h_i}\mathcal{G}^L_{\tilde{\chi}^0_1\tilde{\chi}^0_\ell Z}, \tag{B58}$$

$$\Lambda_{LRL} = \mathcal{G}^L_{\tilde{\chi}^0_1\tilde{\chi}^0_n Z}\mathcal{G}^R_{\tilde{\chi}^0_\ell\tilde{\chi}^0_n h_i}\mathcal{G}^{L*}_{\tilde{\chi}^0_1\tilde{\chi}^0_\ell Z},$$
$$\Lambda_{LRR} = -\mathcal{G}^L_{\tilde{\chi}^0_1\tilde{\chi}^0_n Z}\mathcal{G}^R_{\tilde{\chi}^0_\ell\tilde{\chi}^0_n h_i}\mathcal{G}^L_{\tilde{\chi}^0_1\tilde{\chi}^0_\ell Z}, \tag{B59}$$

$$\Lambda_{RLL} = \mathcal{G}^R_{\tilde{\chi}^0_1\tilde{\chi}^0_n Z}\mathcal{G}^L_{\tilde{\chi}^0_\ell\tilde{\chi}^0_n h_i}\mathcal{G}^{L*}_{\tilde{\chi}^0_1\tilde{\chi}^0_\ell Z},$$
$$\Lambda_{RLR} = -\mathcal{G}^R_{\tilde{\chi}^0_1\tilde{\chi}^0_n Z}\mathcal{G}^L_{\tilde{\chi}^0_\ell\tilde{\chi}^0_n h_i}\mathcal{G}^L_{\tilde{\chi}^0_1\tilde{\chi}^0_\ell Z}, \tag{B60}$$

$$\Lambda_{RRL} = \mathcal{G}^R_{\tilde{\chi}^0_1\tilde{\chi}^0_n Z}\mathcal{G}^R_{\tilde{\chi}^0_\ell\tilde{\chi}^0_n h_i}\mathcal{G}^{L*}_{\tilde{\chi}^0_1\tilde{\chi}^0_\ell Z},$$
$$\Lambda_{RRR} = -\mathcal{G}^R_{\tilde{\chi}^0_1\tilde{\chi}^0_n Z}\mathcal{G}^R_{\tilde{\chi}^0_\ell\tilde{\chi}^0_n h_i}\mathcal{G}^L_{\tilde{\chi}^0_1\tilde{\chi}^0_\ell Z}, \tag{B61}$$

where $\mathcal{G}^L_{\tilde{\chi}^0_\ell\tilde{\chi}^0_n Z} = \frac{g_2}{c_W}N^L_{\ell n}$ and $\mathcal{G}^R_{\tilde{\chi}^0_\ell\tilde{\chi}^0_n Z} = \frac{g_2}{c_W}N^R_{\ell n}$.

(2) $h_i = h_1/h_2$, $F = \tilde{\chi}^\pm_\ell$, $F' = \tilde{\chi}^\pm_n$, $V = W^\pm$.

$$\Lambda_{LLL} = \mathcal{G}^L_{\tilde{\chi}^0_1\tilde{\chi}^\pm_n W^\pm}\mathcal{G}^L_{\tilde{\chi}^\pm_\ell\tilde{\chi}^\pm_n h_i}\mathcal{G}^{R*}_{\tilde{\chi}^0_1\tilde{\chi}^\pm_\ell W^\pm},$$
$$\Lambda_{LLR} = \mathcal{G}^L_{\tilde{\chi}^0_1\tilde{\chi}^\pm_n W^\pm}\mathcal{G}^L_{\tilde{\chi}^\pm_\ell\tilde{\chi}^\pm_n h_i}\mathcal{G}^{L*}_{\tilde{\chi}^0_1\tilde{\chi}^\pm_\ell W^\pm}, \tag{B62}$$

$$\Lambda_{LRL} = \mathcal{G}^L_{\tilde{\chi}^0_1\tilde{\chi}^\pm_n W^\pm}\mathcal{G}^R_{\tilde{\chi}^\pm_\ell\tilde{\chi}^\pm_n h_i}\mathcal{G}^{R*}_{\tilde{\chi}^0_1\tilde{\chi}^\pm_\ell W^\pm},$$
$$\Lambda_{LRR} = \mathcal{G}^L_{\tilde{\chi}^0_1\tilde{\chi}^\pm_n W^\pm}\mathcal{G}^R_{\tilde{\chi}^\pm_\ell\tilde{\chi}^\pm_n h_i}\mathcal{G}^{L*}_{\tilde{\chi}^0_1\tilde{\chi}^\pm_\ell W^\pm}, \tag{B63}$$

$$\Lambda_{RLL} = \mathcal{G}^R_{\tilde{\chi}^0_1\tilde{\chi}^\pm_n W^\pm}\mathcal{G}^L_{\tilde{\chi}^\pm_\ell\tilde{\chi}^\pm_n h_i}\mathcal{G}^{R*}_{\tilde{\chi}^0_1\tilde{\chi}^\pm_\ell W^\pm},$$
$$\Lambda_{RLR} = \mathcal{G}^R_{\tilde{\chi}^0_1\tilde{\chi}^\pm_n W^\pm}\mathcal{G}^L_{\tilde{\chi}^\pm_\ell\tilde{\chi}^\pm_n h_i}\mathcal{G}^{L*}_{\tilde{\chi}^0_1\tilde{\chi}^\pm_\ell W^\pm}, \tag{B64}$$

$$\Lambda_{RRL} = \mathcal{G}^R_{\tilde{\chi}^0_1\tilde{\chi}^\pm_n W^\pm}\mathcal{G}^R_{\tilde{\chi}^\pm_\ell\tilde{\chi}^\pm_n h_i}\mathcal{G}^{R*}_{\tilde{\chi}^0_1\tilde{\chi}^\pm_\ell W^\pm},$$
$$\Lambda_{RRR} = \mathcal{G}^R_{\tilde{\chi}^0_1\tilde{\chi}^\pm_n W^\pm}\mathcal{G}^R_{\tilde{\chi}^\pm_\ell\tilde{\chi}^\pm_n h_i}\mathcal{G}^{L*}_{\tilde{\chi}^0_1\tilde{\chi}^\pm_\ell W^\pm}, \tag{B65}$$

where $\mathcal{G}^L_{\tilde{\chi}^0_\ell\tilde{\chi}^\pm_n W^\pm} = g_2 C^L_{\ell n}$ and $\mathcal{G}^R_{\tilde{\chi}^0_\ell\tilde{\chi}^\pm_n W^\pm} = g_2 C^R_{\ell n}$.

4. Topology-(2b)

The respective Feynman diagram is shown in Fig. 6(b).

$$\begin{aligned} i\delta\Gamma^{(d)} = -\frac{i}{16\pi^2}[&P_L\{\eta_{LL}m_{\tilde{\chi}^0_1}(d-2)\mathbf{C}_2 \\ &+ \eta_{RL}m_F d\mathbf{C}_0 + \eta_{RR}m_{\tilde{\chi}^0_1}(d-2)\mathbf{C}_1\} \\ &+ P_R\{\eta_{LL}m_{\tilde{\chi}^0_1}(d-2)\mathbf{C}_1 + \eta_{LR}m_F d\mathbf{C}_0 \\ &+ \eta_{RR}m_{\tilde{\chi}^0_1}(d-2)\mathbf{C}_2\}], \end{aligned} \tag{B66}$$

where $\mathbf{C}_i = \mathbf{C}_i(m^2_{\tilde{\chi}^0_1}, q^2, m^2_{\tilde{\chi}^0_1}; m_F, m_V, m_V)$ and

$$\eta_{LL} = \mathcal{G}_{VVh_i}\mathcal{G}^L_{\tilde{\chi}^0_1 FV}\mathcal{G}^L_{\tilde{\chi}^0_1 FV},$$
$$\eta_{LR} = \mathcal{G}_{VVh_i}\mathcal{G}^L_{\tilde{\chi}^0_1 FV}\mathcal{G}^R_{\tilde{\chi}^0_1 FV}, \tag{B67}$$

$$\eta_{RL} = \mathcal{G}_{VVh_i}\mathcal{G}^R_{\tilde{\chi}^0_1 FV}\mathcal{G}^L_{\tilde{\chi}^0_1 FV},$$
$$\eta_{RR} = \mathcal{G}_{VVh_i}\mathcal{G}^R_{\tilde{\chi}^0_1 FV}\mathcal{G}^R_{\tilde{\chi}^0_1 FV}. \tag{B68}$$

(1) $h_i = h_1/h_2$, $F = \tilde{\chi}^0_\ell$, $V = Z$.

$$\eta_{LL} = \mathcal{G}_{ZZh_i}\mathcal{G}^L_{\tilde{\chi}^0_1\tilde{\chi}^0_\ell Z}\mathcal{G}^{L*}_{\tilde{\chi}^0_1\tilde{\chi}^0_\ell Z},$$
$$\eta_{LR} = -\mathcal{G}_{ZZh_i}\mathcal{G}^L_{\tilde{\chi}^0_1\tilde{\chi}^0_\ell Z}\mathcal{G}^L_{\tilde{\chi}^0_1\tilde{\chi}^0_\ell Z}, \tag{B69}$$

$$\eta_{RL} = \mathcal{G}_{ZZh_i}\mathcal{G}^R_{\tilde{\chi}^0_1\tilde{\chi}^0_\ell Z}\mathcal{G}^{L*}_{\tilde{\chi}^0_1\tilde{\chi}^0_\ell Z},$$
$$\eta_{RR} = -\mathcal{G}_{ZZh_i}\mathcal{G}^R_{\tilde{\chi}^0_1\tilde{\chi}^0_\ell Z}\mathcal{G}^L_{\tilde{\chi}^0_1\tilde{\chi}^0_\ell Z}, \tag{B70}$$

where $\mathcal{G}_{ZZh_i} = g_2 M_Z g^{\mu\nu} Y_{h_i}$, with $Y_{h_i} = \begin{cases} \frac{s_{\beta-\alpha}}{c_W}; & h_i = h_1 \\ \frac{c_{\beta-\alpha}}{c_W}; & h_i = h_2 \end{cases}$.

(2) $h_i = h_1/h_2$, $F = \tilde{\chi}^\pm_\ell$, $V = W^\pm$.

$$\eta_{LL} = \mathcal{G}_{W^\pm W^\pm h_i}\mathcal{G}^L_{\tilde{\chi}^0_1\tilde{\chi}^\pm_\ell W^\pm}\mathcal{G}^{R*}_{\tilde{\chi}^0_1\tilde{\chi}^\pm_\ell W^\pm},$$
$$\eta_{LR} = \mathcal{G}_{W^\pm W^\pm h_i}\mathcal{G}^L_{\tilde{\chi}^0_1\tilde{\chi}^\pm_\ell W^\pm}\mathcal{G}^{L*}_{\tilde{\chi}^0_1\tilde{\chi}^\pm_\ell W^\pm}, \tag{B71}$$

$$\eta_{RL} = \mathcal{G}_{W^\pm W^\pm h_i}\mathcal{G}^R_{\tilde{\chi}^0_1\tilde{\chi}^\pm_\ell W^\pm}\mathcal{G}^{R*}_{\tilde{\chi}^0_1\tilde{\chi}^\pm_\ell W^\pm},$$
$$\eta_{RR} = \mathcal{G}_{W^\pm W^\pm h_i}\mathcal{G}^R_{\tilde{\chi}^0_1\tilde{\chi}^\pm_\ell W^\pm}\mathcal{G}^{L*}_{\tilde{\chi}^0_1\tilde{\chi}^\pm_\ell W^\pm}, \tag{B72}$$

where $\mathcal{G}_{W^\pm W^\pm h_i} = g_2 M_W g^{\mu\nu} Y'_{h_i}$, with $Y'_{h_i} = \begin{cases} s_{\beta-\alpha}; & h_i = h_1 \\ c_{\beta-\alpha}; & h_i = h_2 \end{cases}$.

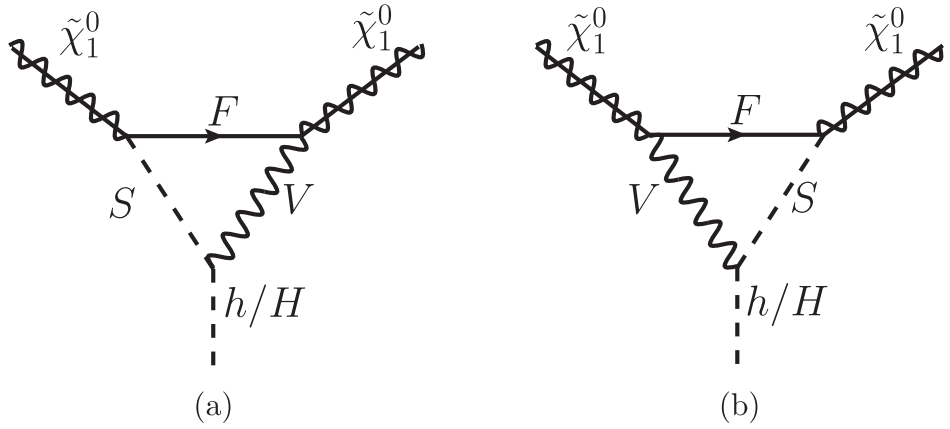

FIG. 7. Topology 3(a) and 3(b).

5. Topology-(3a)

The respective Feynman diagram is shown in Fig. 7(a).

$$\begin{aligned} i\delta\Gamma^{(e)} = \frac{i}{16\pi^2}[&P_L\{\psi_{LL} m_{\tilde{\chi}_1^0} m_F(\mathbf{C}_2 - \mathbf{C}_0) + \psi_{LR} m^2_{\tilde{\chi}_1^0}(\mathbf{C}_1 + 2\mathbf{C}_2) + \psi_{RL}\{-d\mathbf{C}_{00} \\ &- m^2_{\tilde{\chi}_1^0}(\mathbf{C}_{22} + 2\mathbf{C}_{12} + \mathbf{C}_{11} + 2\mathbf{C}_1) + q^2\mathbf{C}_{12} + (2q^2 - 3m^2_{\tilde{\chi}_1^0})\mathbf{C}_2\} \\ &+ \psi_{RR} m_{\tilde{\chi}_1^0} m_F(\mathbf{C}_1 + 2\mathbf{C}_0)\} + P_R\{\psi_{LL} m_{\tilde{\chi}_1^0} m_F(\mathbf{C}_1 + 2\mathbf{C}_0) \\ &+ \psi_{LR}\{-d\mathbf{C}_{00} - m^2_{\tilde{\chi}_1^0}(\mathbf{C}_{22} + 2\mathbf{C}_{12} + \mathbf{C}_{11} + 2\mathbf{C}_1) + q^2\mathbf{C}_{12} + (2q^2 - 3m^2_{\tilde{\chi}_1^0})\mathbf{C}_2\} \\ &+ \psi_{RL} m^2_{\tilde{\chi}_1^0}(\mathbf{C}_1 + 2\mathbf{C}_2) + \psi_{RR} m_{\tilde{\chi}_1^0} m_F(\mathbf{C}_2 - \mathbf{C}_0)\}], \end{aligned} \tag{B73}$$

where $\mathbf{C}_i = \mathbf{C}_i(m^2_{\tilde{\chi}_1^0}, q^2, m^2_{\tilde{\chi}_1^0}; m_F, m_S, m_V)$, $\mathbf{C}_{ij} = \mathbf{C}_{ij}(m^2_{\tilde{\chi}_1^0}, q^2, m^2_{\tilde{\chi}_1^0}; m_F, m_S, m_V)$ and

$$\begin{aligned} \psi_{LL} &= \mathcal{G}_{h_i SV}\mathcal{G}^L_{\tilde{\chi}_1^0 FV}\mathcal{G}^L_{\tilde{\chi}_1^0 FS}, \\ \psi_{LR} &= \mathcal{G}_{h_i SV}\mathcal{G}^L_{\tilde{\chi}_1^0 FV}\mathcal{G}^R_{\tilde{\chi}_1^0 FS}, \end{aligned} \tag{B74}$$

$$\begin{aligned} \psi_{RL} &= \mathcal{G}_{h_i SV}\mathcal{G}^R_{\tilde{\chi}_1^0 FV}\mathcal{G}^L_{\tilde{\chi}_1^0 FS}, \\ \psi_{RR} &= \mathcal{G}_{h_i SV}\mathcal{G}^R_{\tilde{\chi}_1^0 FV}\mathcal{G}^R_{\tilde{\chi}_1^0 FS}. \end{aligned} \tag{B75}$$

(1) $h_i = h_1/h_2$, $F = \tilde{\chi}^0_\ell$, $S = A$, $V = Z$.

$$\begin{aligned} \psi_{LL} &= \mathcal{G}_{h_i AZ}\mathcal{G}^L_{\tilde{\chi}_1^0\tilde{\chi}^0_\ell Z}\mathcal{G}^{R*}_{\tilde{\chi}_1^0\tilde{\chi}^0_\ell A}, \\ \psi_{LR} &= \mathcal{G}_{h_i AZ}\mathcal{G}^L_{\tilde{\chi}_1^0\tilde{\chi}^0_\ell Z}\mathcal{G}^{L*}_{\tilde{\chi}_1^0\tilde{\chi}^0_\ell A}, \end{aligned} \tag{B76}$$

$$\begin{aligned} \psi_{RL} &= \mathcal{G}_{h_i AZ}\mathcal{G}^R_{\tilde{\chi}_1^0\tilde{\chi}^0_\ell Z}\mathcal{G}^{R*}_{\tilde{\chi}_1^0\tilde{\chi}^0_\ell A}, \\ \psi_{RR} &= \mathcal{G}_{h_i AZ}\mathcal{G}^R_{\tilde{\chi}_1^0\tilde{\chi}^0_\ell Z}\mathcal{G}^{L*}_{\tilde{\chi}_1^0\tilde{\chi}^0_\ell A}, \end{aligned} \tag{B77}$$

where $\mathcal{G}_{h_i AZ} = \frac{g_2}{2c_W} Y''_{h_i}$, with $Y''_{h_i} = \begin{cases} c_{\beta-\alpha}; & h_i = h_1 \\ -s_{\beta-\alpha}; & h_i = h_2 \end{cases}$.

(2) $h_i = h_1/h_2$, $F = \tilde{\chi}^0_\ell$, $S = G$, $V = Z$.

$$\begin{aligned} \psi_{LL} &= \mathcal{G}_{h_i GZ}\mathcal{G}^L_{\tilde{\chi}_1^0\tilde{\chi}^0_\ell Z}\mathcal{G}^{R*}_{\tilde{\chi}_1^0\tilde{\chi}^0_\ell G}, \\ \psi_{LR} &= \mathcal{G}_{h_i GZ}\mathcal{G}^L_{\tilde{\chi}_1^0\tilde{\chi}^0_\ell Z}\mathcal{G}^{L*}_{\tilde{\chi}_1^0\tilde{\chi}^0_\ell G}, \end{aligned} \tag{B78}$$

$$\begin{aligned} \psi_{RL} &= \mathcal{G}_{h_i GZ}\mathcal{G}^R_{\tilde{\chi}_1^0\tilde{\chi}^0_\ell Z}\mathcal{G}^{R*}_{\tilde{\chi}_1^0\tilde{\chi}^0_\ell G}, \\ \psi_{RR} &= \mathcal{G}_{h_i GZ}\mathcal{G}^R_{\tilde{\chi}_1^0\tilde{\chi}^0_\ell Z}\mathcal{G}^{L*}_{\tilde{\chi}_1^0\tilde{\chi}^0_\ell G}, \end{aligned} \tag{B79}$$

where

$$\mathcal{G}_{h_i GZ} = \begin{cases} \frac{g_2}{2c_W} s_{\beta-\alpha}; & h_i = h_1 \\ \frac{g_2}{2c_W} c_{\beta-\alpha}; & h_i = h_2 \end{cases}.$$

(3) $h_i = h_1/h_2$, $F = \tilde{\chi}^\pm_\ell$, $S = H^\pm$, $V = W^\pm$.

$$\begin{aligned} \psi_{LL} &= \mathcal{G}_{h_i H^\pm W^\pm}\mathcal{G}^L_{\tilde{\chi}_1^0\tilde{\chi}^\pm_\ell W^\pm}\mathcal{G}^{R*}_{\tilde{\chi}_1^0\tilde{\chi}^\pm_\ell H^\pm}, \\ \psi_{LR} &= \mathcal{G}_{h_i H^\pm W^\pm}\mathcal{G}^L_{\tilde{\chi}_1^0\tilde{\chi}^\pm_\ell W^\pm}\mathcal{G}^{L*}_{\tilde{\chi}_1^0\tilde{\chi}^\pm_\ell H^\pm}, \end{aligned} \tag{B80}$$

$$\psi_{RL} = \mathcal{G}_{h_i H^\pm W^\pm} \mathcal{G}^R_{\tilde{\chi}^0_1 \tilde{\chi}^\pm_\ell W^\pm} \mathcal{G}^{R*}_{\tilde{\chi}^0_1 \tilde{\chi}^\pm_\ell H^\pm},$$
$$\psi_{RR} = \mathcal{G}_{h_i H^\pm W^\pm} \mathcal{G}^R_{\tilde{\chi}^0_1 \tilde{\chi}^\pm_\ell W^\pm} \mathcal{G}^{L*}_{\tilde{\chi}^0_1 \tilde{\chi}^\pm_\ell H^\pm}, \quad \text{(B81)}$$

where $\mathcal{G}_{h_i H^\pm W^\pm} = \frac{g_2}{2} Y''_{h_i}$.

(4) $h_i = h_1/h_2$, $F = \tilde{\chi}^\pm_\ell$, $S = G^\pm$, $V = W^\pm$.

$$\psi_{LL} = \mathcal{G}_{h_i G^\pm W^\pm} \mathcal{G}^L_{\tilde{\chi}^0_1 \tilde{\chi}^\pm_\ell W^\pm} \mathcal{G}^{R*}_{\tilde{\chi}^0_1 \tilde{\chi}^\pm_\ell G^\pm},$$
$$\psi_{LR} = \mathcal{G}_{h_i G^\pm W^\pm} \mathcal{G}^L_{\tilde{\chi}^0_1 \tilde{\chi}^\pm_\ell W^\pm} \mathcal{G}^{L*}_{\tilde{\chi}^0_1 \tilde{\chi}^\pm_\ell G^\pm}, \quad \text{(B82)}$$

$$\psi_{RL} = \mathcal{G}_{h_i G^\pm W^\pm} \mathcal{G}^R_{\tilde{\chi}^0_1 \tilde{\chi}^\pm_\ell W^\pm} \mathcal{G}^{R*}_{\tilde{\chi}^0_1 \tilde{\chi}^\pm_\ell G^\pm},$$
$$\psi_{RR} = \mathcal{G}_{h_i G^\pm W^\pm} \mathcal{G}^R_{\tilde{\chi}^0_1 \tilde{\chi}^\pm_\ell W^\pm} \mathcal{G}^{L*}_{\tilde{\chi}^0_1 \tilde{\chi}^\pm_\ell G^\pm}, \quad \text{(B83)}$$

where

$$\mathcal{G}_{h_i G^\pm W^\pm} = \begin{cases} -\frac{g_2}{2} s_{\beta-\alpha}; & h_i = h_1 \\ -\frac{g_2}{2} c_{\beta-\alpha}; & h_i = h_2 \end{cases}.$$

6. Topology-(3b)

The respective Feynman diagram is shown in Fig. 7(b).

$$i\delta\Gamma^{(f)} = \frac{i}{16\pi^2}[P_L\{\Xi_{LL}\{d\mathbf{C}_{00} + m^2_{\tilde{\chi}^0_1}(\mathbf{C}_{22} + 2\mathbf{C}_{12} + \mathbf{C}_{11} + 2\mathbf{C}_2 + 3\mathbf{C}_1) - q^2(\mathbf{C}_{12} + 2\mathbf{C}_1)\} + \Xi_{LR} m_{\tilde{\chi}^0_1} m_F(\mathbf{C}_0 - \mathbf{C}_1)$$
$$- \Xi_{RL} m_{\tilde{\chi}^0_1} m_F(\mathbf{C}_2 + 2\mathbf{C}_0) - \Xi_{RR} m^2_{\tilde{\chi}^0_1}(\mathbf{C}_2 + 2\mathbf{C}_1)\} + P_R\{-\Xi_{LL} m^2_{\tilde{\chi}^0_1}(\mathbf{C}_2 + 2\mathbf{C}_1) - \Xi_{LR} m_{\tilde{\chi}^0_1} m_F(\mathbf{C}_2 + 2\mathbf{C}_0)$$
$$+ \Xi_{RL} m_{\tilde{\chi}^0_1} m_F(\mathbf{C}_0 - \mathbf{C}_1) + \Xi_{RR}\{d\mathbf{C}_{00} + m^2_{\tilde{\chi}^0_1}(\mathbf{C}_{22} + 2\mathbf{C}_{12} + \mathbf{C}_{11} + 2\mathbf{C}_2 + 3\mathbf{C}_1) - q^2(\mathbf{C}_{12} + 2\mathbf{C}_1)\}\}], \quad \text{(B84)}$$

where $\mathbf{C}_i = \mathbf{C}_i(m^2_{\tilde{\chi}^0_1}, q^2, m^2_{\tilde{\chi}^0_1}; m_F, m_V, m_S)$, $\mathbf{C}_{ij} = \mathbf{C}_{ij}(m^2_{\tilde{\chi}^0_1}, q^2, m^2_{\tilde{\chi}^0_1}; m_F, m_V, m_S)$ and

$$\Xi_{LL} = \mathscr{G}_{h_i SV} \mathscr{G}^L_{\tilde{\chi}^0_1 FS} \mathscr{G}^L_{\tilde{\chi}^0_1 FV},$$
$$\Xi_{LR} = \mathscr{G}_{h_i SV} \mathscr{G}^L_{\tilde{\chi}^0_1 FS} \mathscr{G}^R_{\tilde{\chi}^0_1 FV}, \quad \text{(B85)}$$

$$\Xi_{RL} = \mathscr{G}_{h_i SV} \mathscr{G}^R_{\tilde{\chi}^0_1 FS} \mathscr{G}^L_{\tilde{\chi}^0_1 FV},$$
$$\Xi_{RR} = \mathscr{G}_{h_i SV} \mathscr{G}^R_{\tilde{\chi}^0_1 FS} \mathscr{G}^R_{\tilde{\chi}^0_1 FV}. \quad \text{(B86)}$$

(1) $h_i = h_1/h_2$, $F = \tilde{\chi}^0_\ell$, $S = A$, $V = Z$.

$$\Xi_{LL} = \mathcal{G}_{h_i AZ} \mathcal{G}^L_{\tilde{\chi}^0_1 \tilde{\chi}^0_\ell A} \mathcal{G}^{L*}_{\tilde{\chi}^0_1 \tilde{\chi}^0_\ell Z},$$
$$\Xi_{LR} = -\mathcal{G}_{h_i AZ} \mathcal{G}^L_{\tilde{\chi}^0_1 \tilde{\chi}^0_\ell A} \mathcal{G}^L_{\tilde{\chi}^0_1 \tilde{\chi}^0_\ell Z}, \quad \text{(B87)}$$

$$\Xi_{RL} = \mathcal{G}_{h_i AZ} \mathcal{G}^R_{\tilde{\chi}^0_1 \tilde{\chi}^0_\ell A} \mathcal{G}^{L*}_{\tilde{\chi}^0_1 \tilde{\chi}^0_\ell Z},$$
$$\Xi_{RR} = -\mathcal{G}_{h_i AZ} \mathcal{G}^R_{\tilde{\chi}^0_1 \tilde{\chi}^0_\ell A} \mathcal{G}^L_{\tilde{\chi}^0_1 \tilde{\chi}^0_\ell Z}. \quad \text{(B88)}$$

(2) $h_i = h_1/h_2$, $F = \tilde{\chi}^0_\ell$, $S = G$, $V = Z$.

$$\Xi_{LL} = \mathcal{G}_{h_i GZ} \mathcal{G}^L_{\tilde{\chi}^0_1 \tilde{\chi}^0_\ell G} \mathcal{G}^{L*}_{\tilde{\chi}^0_1 \tilde{\chi}^0_\ell Z},$$
$$\Xi_{LR} = -\mathcal{G}_{h_i GZ} \mathcal{G}^L_{\tilde{\chi}^0_1 \tilde{\chi}^0_\ell G} \mathcal{G}^L_{\tilde{\chi}^0_1 \tilde{\chi}^0_\ell Z}, \quad \text{(B89)}$$

$$\Xi_{RL} = \mathcal{G}_{h_i GZ} \mathcal{G}^R_{\tilde{\chi}^0_1 \tilde{\chi}^0_\ell G} \mathcal{G}^{L*}_{\tilde{\chi}^0_1 \tilde{\chi}^0_\ell Z},$$
$$\Xi_{RR} = -\mathcal{G}_{h_i GZ} \mathcal{G}^R_{\tilde{\chi}^0_1 \tilde{\chi}^0_\ell G} \mathcal{G}^L_{\tilde{\chi}^0_1 \tilde{\chi}^0_\ell Z}. \quad \text{(B90)}$$

(3) $h_i = h_1/h_2$, $F = \tilde{\chi}^\pm_\ell$, $S = H^\pm$, $V = W^\pm$.

$$\Xi_{LL} = \mathcal{G}_{h_i H^\pm W^\pm} \mathcal{G}^L_{\tilde{\chi}^0_1 \tilde{\chi}^\pm_\ell H^\pm} \mathcal{G}^{R*}_{\tilde{\chi}^0_1 \tilde{\chi}^\pm_\ell W^\pm},$$
$$\Xi_{LR} = \mathcal{G}_{h_i H^\pm W^\pm} \mathcal{G}^L_{\tilde{\chi}^0_1 \tilde{\chi}^\pm_\ell H^\pm} \mathcal{G}^{L*}_{\tilde{\chi}^0_1 \tilde{\chi}^\pm_\ell W^\pm}, \quad \text{(B91)}$$

$$\Xi_{RL} = \mathcal{G}_{h_i H^\pm W^\pm} \mathcal{G}^R_{\tilde{\chi}^0_1 \tilde{\chi}^\pm_\ell H^\pm} \mathcal{G}^{R*}_{\tilde{\chi}^0_1 \tilde{\chi}^\pm_\ell W^\pm},$$
$$\Xi_{RR} = \mathcal{G}_{h_i H^\pm W^\pm} \mathcal{G}^R_{\tilde{\chi}^0_1 \tilde{\chi}^\pm_\ell H^\pm} \mathcal{G}^{L*}_{\tilde{\chi}^0_1 \tilde{\chi}^\pm_\ell W^\pm}. \quad \text{(B92)}$$

(4) $h_i = h_1/h_2$, $F = \tilde{\chi}^\pm_\ell$, $S = G^\pm$, $V = W^\pm$.

$$\Xi_{LL} = \mathcal{G}_{h_i G^\pm W^\pm} \mathcal{G}^L_{\tilde{\chi}^0_1 \tilde{\chi}^\pm_\ell G^\pm} \mathcal{G}^{R*}_{\tilde{\chi}^0_1 \tilde{\chi}^\pm_\ell W^\pm},$$
$$\Xi_{LR} = \mathcal{G}_{h_i G^\pm W^\pm} \mathcal{G}^L_{\tilde{\chi}^0_1 \tilde{\chi}^\pm_\ell G^\pm} \mathcal{G}^{L*}_{\tilde{\chi}^0_1 \tilde{\chi}^\pm_\ell W^\pm}, \quad \text{(B93)}$$

$$\Xi_{RL} = \mathcal{G}_{h_i G^\pm W^\pm} \mathcal{G}^R_{\tilde{\chi}^0_1 \tilde{\chi}^\pm_\ell G^\pm} \mathcal{G}^{R*}_{\tilde{\chi}^0_1 \tilde{\chi}^\pm_\ell W^\pm},$$
$$\Xi_{RR} = \mathcal{G}_{h_i G^\pm W^\pm} \mathcal{G}^R_{\tilde{\chi}^0_1 \tilde{\chi}^\pm_\ell G^\pm} \mathcal{G}^{L*}_{\tilde{\chi}^0_1 \tilde{\chi}^\pm_\ell W^\pm}. \quad \text{(B94)}$$

In the above, we have used the following [65]:

$$C^L_{\ell k} = N_{\ell 2}V^*_{k1} - \frac{1}{\sqrt{2}}N_{\ell 4}V^*_{k2},$$
$$C^R_{\ell k} = N^*_{\ell 2}U_{k1} + \frac{1}{\sqrt{2}}N^*_{\ell 3}U_{k2},$$
$$\mathcal{N}^L_{\ell n} = \frac{1}{2}(-N_{\ell 3}N^*_{n3} + N_{\ell 4}N^*_{n4}),$$
$$\mathcal{N}^R_{\ell n} = -(\mathcal{N}^L_{\ell n})^*,$$
$$Q_{k\ell} = \frac{1}{2}V_{k1}U_{\ell 2},$$
$$S_{k\ell} = \frac{1}{2}V_{k2}U_{\ell 1},$$
$$Q'^L_{\ell k} = c_\beta\left[N^*_{\ell 4}V^*_{k1} + \frac{1}{\sqrt{2}}V^*_{k2}(N^*_{\ell 2} + t_W N^*_{\ell 1})\right],$$
$$Q'^R_{\ell k} = s_\beta\left[N_{\ell 3}U_{k1} - \frac{1}{\sqrt{2}}U_{k2}(N_{\ell 2} + t_W N_{\ell 1})\right],$$
$$Q''_{n\ell} = \frac{1}{2}[N_{n3}(N_{\ell 2} - t_W N_{\ell 1}) + N_{\ell 3}(N_{n2} - t_W N_{n1})],$$
$$S''_{n\ell} = \frac{1}{2}[N_{n4}(N_{\ell 2} - t_W N_{\ell 1}) + N_{\ell 4}(N_{n2} - t_W N_{n1})].$$

APPENDIX C

The counterterm Lagrangian for the $\tilde{\chi}^0_1 - \tilde{\chi}^0_1 - h_i$ interaction ($\mathscr{L}_{\rm CT}$) is given as follows:

$$\mathscr{L}_{\rm CT} \supset -\frac{1}{2}h_1\bar{\tilde{\chi}}^0_1(\delta\mathcal{C}^R_1 P_R + \delta\mathscr{C}^L_1 P_L)\tilde{\chi}^0_1 - \frac{1}{2}h_2\bar{\tilde{\chi}}^0_1(\delta\mathscr{C}^R_2 P_R + \delta\mathscr{C}^L_2 P_L)\tilde{\chi}^0_1,$$

where $\delta\mathscr{C}^L_i = \delta\mathscr{C}^{R*}_i$ for $i \in \{1,2\}$.

In the above expression, $\delta\mathcal{C}^R_1$ is given by

$$\delta\mathscr{C}^R_1 = -\frac{e}{4s^2_{\rm W}}\left(\frac{2}{c^3_{\rm W}}A_1 + B_1\frac{s_{\rm W}}{c_{\rm W}}\right), \tag{C1}$$

where A_1 and B_1 are given by

$$A_1 = -2(s_\alpha N_{13} + c_\alpha {\rm N}_{14})(({\rm \delta Z_e}s_{\rm W} - \delta s_{\rm W}){\rm N}_{12}c^3_{\rm W} - {\rm N}_{11}(\delta s_{\rm W}s_{\rm W} + {\rm \delta Z_e}c^2_{\rm W})s^2_{\rm W}),$$
$$B_1 = \sum_{i=1}^{4}((s_\alpha N_{i3} + c_\alpha N_{i4})(s_{\rm W}N_{11} - c_{\rm W}N_{12}) + (s_{\rm W}N_{i1} - c_{\rm W}N_{i2})(s_\alpha N_{13} + c_\alpha N_{14}))(\delta Z^*_{1i} + \delta Z^*_{i1}) + 2((\delta Z^{\rm H}_{11}s_\alpha - \delta Z^{\rm H}_{12}c_\alpha)N_{13} + (\delta Z^{\rm H}_{11}c_\alpha + \delta Z^{\rm H}_{12}s_\alpha)N_{14})(s_{\rm W}N_{11} - c_{\rm W}N_{12}). \tag{C2}$$

In these expressions $s_{\rm W} = \sin\theta_{\rm W}$, $c_{\rm W} = \cos\theta_{\rm W}$, where $\theta_{\rm W}$ is the Weinberg angle, $\delta s_{\rm W}$ and $\delta c_{\rm W}$ denote the respective counterterms. Further, $c_\alpha = \cos\alpha$, $s_\alpha = \sin\alpha$, where α is the mixing angle in the CP-even Higgs boson sector, $\delta {\rm Z_e}$ denotes the counterterm corresponding to the charge e.

We use the following abbreviations in this section. $\widetilde{\rm Re}$ takes the real part of loop integrals but does not affect the complex couplings. For the notations, we have closely followed [107] and [73]. The relevant counterterms have been listed below.

For the Higgs sector, the following counterterms are relevant [107]:

$$\delta Z_{H_1} = -{\rm Re}\Sigma'_{h_2}(0)|_{\alpha=0,{\rm div}},$$
$$\delta Z_{H_2} = -{\rm Re}\Sigma'_{h_1}(0)|_{\alpha=0,{\rm div}},$$
$$\delta t_\beta = \frac{1}{2}t_\beta(\delta Z_{H_2} - \delta Z_{H_1}).$$

In the gauge boson sector, the relevant counterterms are as follows [107]:

$$\delta M^2_Z = \widetilde{\rm Re}\Sigma^T_Z(M^2_Z),$$
$$\delta M^2_W = \widetilde{\rm Re}\Sigma^T_W(M^2_W),$$
$$\delta Z_{\gamma\gamma} = -\widetilde{\rm Re}\Sigma'^T_\gamma(0),$$
$$\delta Z_{Z\gamma} = \frac{2}{M^2_Z}\widetilde{\rm Re}\Sigma^T_{\gamma Z}(0),$$
$$\delta s_{\rm w} = \frac{1}{2}\frac{c^2_{\rm w}}{s_{\rm w}}\left(\frac{\delta M^2_Z}{M^2_Z} - \frac{\delta M^2_W}{M^2_W}\right),$$
$$\delta Z_e = \frac{1}{2}\left(\frac{s_{\rm w}}{c_{\rm w}}\delta Z_{Z\gamma} - \delta Z_{\gamma\gamma}\right).$$

The counterterms to the gaugino and Higgsino mass parameters are determined from the chargino-neutralino sector. In the In the CCN(n) scheme, these are given by [73,74,107,111]

$$\delta M_1 = \frac{1}{N^{*2}_{n1}}\{\delta m^{\rm OS}_{\tilde{\chi}^0_n} + \delta N_n - N^{*2}_{n2}\delta M_2 + 2N^*_{n3}N^*_{n4}\delta\mu\}, \tag{C3}$$

$$\delta M_2 = \frac{1}{k_o r_o - k_d r_d}\Big\{U^*_{12}V^*_{12}\delta m^{\rm OS}_{\tilde{\chi}^\pm_2} - U^*_{22}V^*_{22}\delta m^{\rm OS}_{\tilde{\chi}^\pm_1} + \sqrt{2}(c_\beta(k_d - k_o)V^*_{12}V^*_{22} + s_\beta(r_o - r_d)U^*_{12}U^*_{22})M_W c^2_\beta\delta t_\beta + (s_\beta(k_d - k_o)V^*_{12}V^*_{22} - c_\beta(r_o - r_d)U^*_{12}U^*_{22})\frac{\delta M^2_W}{\sqrt{2}M_W}\Big\}, \tag{C4}$$

$$\delta\mu = \frac{1}{k_o r_o - k_d r_d}\Big\{U^*_{21}V^*_{21}\delta m^{\rm OS}_{\tilde{\chi}^\pm_1} - U^*_{11}V^*_{11}\delta m^{\rm OS}_{\tilde{\chi}^\pm_2} - \sqrt{2}(s_\beta(k_d - k_o)V^*_{11}V^*_{21} + c_\beta(r_o - r_d)U^*_{11}U^*_{21})M_W c^2_\beta\delta t_\beta + (c_\beta(k_d - k_o)V^*_{11}V^*_{21} - s_\beta(r_o - r_d)U^*_{11}U^*_{21})\frac{\delta M^2_W}{\sqrt{2}M_W}\Big\}, \tag{C5}$$

where we have used the following notations:

$$k_d = U_{11}^* U_{22}^*, \qquad k_o = U_{12}^* U_{21}^*,$$
$$r_d = V_{11}^* V_{22}^*, \qquad r_o = V_{12}^* V_{21}^*,$$

and

$$\delta N_n = 2c_\beta^2 \delta t_\beta (s_\beta N_{n3}^* + c_\beta N_{n4}^*)(M_W N_{n2}^* - M_Z s_w N_{n1}^*) + (c_\beta N_{n3}^* - s_\beta N_{n4}^*)\left(N_{n1}^* \left[\frac{\delta M_Z^2}{M_Z} s_w + 2M_Z \delta s_w\right] - N_{n2}^* \frac{\delta M_W^2}{M_W}\right),$$
$$\delta m_{\tilde{\chi}_n^0}^{OS} = \widetilde{\mathrm{Re}}[m_{\tilde{\chi}_n^0} \Sigma_{\tilde{\chi}^0}^L (m_{\tilde{\chi}_n^0}^2) + \Sigma_{\tilde{\chi}^0}^{SL} (m_{\tilde{\chi}_n^0}^2)]_{nn},$$
$$\delta m_{\tilde{\chi}_c^\pm}^{OS} = \widetilde{\mathrm{Re}}\left[\frac{m_{\tilde{\chi}_c^\pm}}{2}(\Sigma_{\tilde{\chi}^-}^L (m_{\tilde{\chi}_c^\pm}^2) + \Sigma_{\tilde{\chi}^-}^R (m_{\tilde{\chi}_c^\pm}^2)) + \Sigma_{\tilde{\chi}^-}^{SL} (m_{\tilde{\chi}_c^\pm}^2)\right]_{cc}. \tag{C6}$$

We have used $n = 4$ for BP1-4 and $n = 3$ for BP5-6. A more thorough analysis can be found in [73] and [107].

We have used an on shell renormalization scheme, which has been implemented in the FormCalc [107], to evaluate these counterterms for the benchmark scenarios.

Next, $\delta\mathscr{C}_2^R$ is given by

$$\delta\mathscr{C}_2^R = \frac{e}{4s_W^2}\left(\frac{2}{c_W^3} A_2 + B_2 \frac{s_W}{c_W}\right). \tag{C7}$$

In the above expression A_2 and B_2 are given by

$$A_2 = -2(c_\alpha Z_{13} - s_\alpha Z_{14})((\delta Z_e s_W - \delta s_W) Z_{12} c_W^3 - Z_{11}(\delta s_W s_W + \delta Z_e c_W^2) s_W^2),$$
$$B_2 = \sum_{i=1}^{4} [(c_\alpha N_{i3} - s_\alpha N_{i4})(s_W N_{11} - c_W N_{12}) + (s_W N_{i1} - c_W N_{i2})(c_\alpha N_{13} - s_\alpha N_{14})](\delta \bar{Z}_{i1} + \delta Z_{i1}^*)$$
$$+ 2(\delta Z_{22}^H - \delta Z_{12}^H)[s_\alpha (N_{13} - N_{14}) + c_\alpha (N_{13} + N_{14})](s_W N_{11} - c_W N_{12}). \tag{C8}$$

The wavefunction renormalization counterterms for the neutralino sector and the CP-even Higgs sector have been determined using the on shell renormalization scheme [73,115], following the implementation in FormCalc [107]. For different benchmark scenarios, variants of the on shell renormalization scheme have been adopted; a detailed discussion may be found in [74].

[1] R. Barbieri and G. F. Giudice, Upper bounds on supersymmetric particle masses, Nucl. Phys. **B306**, 63 (1988).

[2] J. Ellis, K. Enqvist, D. Nanopoulos, and F. Zwirner, Observables in low-energy superstring models, Mod. Phys. Lett. A **01**, 57 (1986).

[3] K. L. Chan, U. Chattopadhyay, and P. Nath, Naturalness, weak scale supersymmetry and the prospect for the observation of supersymmetry at the Tevatron and at the CERN LHC, Phys. Rev. D **58**, 096004 (1998).

[4] J. L. Feng, Naturalness and the status of supersymmetry, Annu. Rev. Nucl. Part. Sci. **63**, 351 (2013).

[5] G. F. Giudice, Naturalness after LHC8, Proc. Sci. EPS-HEP2013 (**2013**) 163 [arXiv:1307.7879].

[6] H. Baer, V. Barger, P. Huang, D. Mickelson, A. Mustafayev, and X. Tata, Radiative natural supersymmetry: Reconciling electroweak fine-tuning and the Higgs boson mass, Phys. Rev. D **87**, 115028 (2013).

[7] A. Mustafayev and X. Tata, Supersymmetry, naturalness, and light Higgsinos, Indian J. Phys. **88**, 991 (2014).

[8] H. Baer, V. Barger, P. Huang, A. Mustafayev, and X. Tata, Radiative natural SUSY with a 125 GeV Higgs boson, Phys. Rev. Lett. **109**, 161802 (2012).

[9] H. Baer, V. Barger, P. Huang, D. Mickelson, A. Mustafayev, and X. Tata, Naturalness, supersymmetry and light Higgsinos: A snowmass whitepaper, in *Proceedings, Community Summer Study 2013: Snowmass on the*

Mississippi (CSS2013): Minneapolis, MN, USA (2013), arXiv:1306.2926.

[10] K. J. Bae, H. Baer, V. Barger, and D. Sengupta, Revisiting the SUSY μ problem and its solutions in the LHC era, Phys. Rev. D **99**, 115027 (2019).

[11] G. Aad *et al.* (ATLAS Collaboration), Search for charginos and neutralinos in final states with two boosted hadronically decaying bosons and missing transverse momentum in pp collisions at $\sqrt{s} = 13$ TeV with the ATLAS detector, Phys. Rev. D **104**, 112010 (2021).

[12] G. Aad *et al.* (ATLAS Collaboration), Search for chargino-neutralino production with mass splittings near the electroweak scale in three-lepton final states in $\sqrt{s} = 13$ TeV pp collisions with the ATLAS detector, Phys. Rev. D **101**, 072001 (2020).

[13] G. Aad *et al.* (ATLAS Collaboration), Searches for new phenomena in events with two leptons, jets, and missing transverse momentum in 139 fb^{-1} of $\sqrt{s} = 13$ TeV pp collisions with the ATLAS detector, Eur. Phys. J. C **83**, 515 (2023).

[14] G. Aad *et al.* (ATLAS Collaboration), Search for direct pair production of sleptons and charginos decaying to two leptons and neutralinos with mass splittings near the W-boson mass in $\sqrt{s} = 13$ TeV pp collisions with the ATLAS detector, J. High Energy Phys. 06 (2023) 031.

[15] G. Aad *et al.* (ATLAS Collaboration), Search for chargino–neutralino pair production in final states with three leptons and missing transverse momentum in $\sqrt{s} = 13$ TeV pp collisions with the ATLAS detector, Eur. Phys. J. C **81**, 1118 (2021).

[16] A. Tumasyan *et al.* (CMS Collaboration), Search for electroweak production of charginos and neutralinos at $s = 13$ TeV in final states containing hadronic decays of WW, WZ, or WH and missing transverse momentum, Phys. Lett. B **842**, 137460 (2023).

[17] A. Hayrapetyan *et al.* (CMS Collaboration), Search for new physics in multijet events with at least one photon and large missing transverse momentum in proton-proton collisions at 13 TeV, J. High Energy Phys. 10 (2023) 046.

[18] J. L. Feng, K. T. Matchev, and T. Moroi, Multi—TeV scalars are natural in minimal supergravity, Phys. Rev. Lett. **84**, 2322 (2000).

[19] H. Baer, C. Balazs, A. Belyaev, T. Krupovnickas, and X. Tata, Updated reach of the CERN LHC and constraints from relic density, $b \to s\gamma$ and $a(\mu)$ in the mSUGRA model, J. High Energy Phys. 06 (2003) 054.

[20] S. Akula, M. Liu, P. Nath, and G. Peim, Naturalness, supersymmetry and implications for LHC and dark matter, Phys. Lett. B **709**, 192 (2012).

[21] D. Feldman, G. Kane, E. Kuflik, and R. Lu, A new (string motivated) approach to the little hierarchy problem, Phys. Lett. B **704**, 56 (2011).

[22] G. G. Ross, K. Schmidt-Hoberg, and F. Staub, Revisiting fine-tuning in the MSSM, J. High Energy Phys. 03 (2017) 021.

[23] M. Chakraborti, U. Chattopadhyay, A. Choudhury, A. Datta, and S. Poddar, Reduced LHC constraints for Higgsino-like heavier electroweakinos, J. High Energy Phys. 11 (2015) 050.

[24] U. Chattopadhyay, D. Choudhury, M. Drees, P. Konar, and D. P. Roy, Looking for a heavy Higgsino LSP in collider and dark matter experiments, Phys. Lett. B **632**, 114 (2006).

[25] H. Baer, V. Barger, and P. Huang, Hidden SUSY at the LHC: The light Higgsino-world scenario and the role of a lepton collider, J. High Energy Phys. 11 (2011) 031.

[26] T. Han, S. Padhi, and S. Su, Electroweakinos in the light of the Higgs boson, Phys. Rev. D **88**, 115010 (2013).

[27] Z. Han, G. D. Kribs, A. Martin, and A. Menon, Hunting quasidegenerate Higgsinos, Phys. Rev. D **89**, 075007 (2014).

[28] M. Drees and J. S. Kim, Minimal natural supersymmetry after the LHC8, Phys. Rev. D **93**, 095005 (2016).

[29] D. Barducci, A. Belyaev, A. K. M. Bharucha, W. Porod, and V. Sanz, Uncovering natural supersymmetry via the interplay between the LHC and direct dark matter detection, J. High Energy Phys. 07 (2015) 066.

[30] H. Baer, V. Barger, M. Savoy, and X. Tata, Multichannel assault on natural supersymmetry at the high luminosity LHC, Phys. Rev. D **94**, 035025 (2016).

[31] H. Fukuda, N. Nagata, H. Otono, and S. Shirai, Higgsino dark matter or not: Role of disappearing track searches at the LHC and future colliders, Phys. Lett. B **781**, 306 (2018).

[32] R. Mahbubani, P. Schwaller, and J. Zurita, Closing the window for compressed dark sectors with disappearing charged tracks, J. High Energy Phys. 06 (2017) 119; 10 (2017) 061(E).

[33] M. Chakraborti, U. Chattopadhyay, and S. Poddar, How light a Higgsino or a wino dark matter can become in a compressed scenario of MSSM, J. High Energy Phys. 09 (2017) 064.

[34] A. Delgado and M. Quirós, Higgsino dark matter in the MSSM, Phys. Rev. D **103**, 015024 (2021).

[35] H. Baer, V. Barger, and D. Mickelson, Direct and indirect detection of Higgsino-like WIMPs: Concluding the story of electroweak naturalness, Phys. Lett. B **726**, 330 (2013).

[36] C. Dessert, J. W. Foster, Y. Park, B. R. Safdi, and W. L. Xu, Higgsino dark matter confronts 14 years of fermi γ-ray data, Phys. Rev. Lett. **130**, 201001 (2023).

[37] J. Aalbers *et al.* (LZ Collaboration), First dark matter search results from the LUX-ZEPLIN (LZ) experiment, Phys. Rev. Lett. **131**, 041002 (2023).

[38] E. Aprile *et al.* (XENON Collaboration), First dark matter search with nuclear recoils from the XENONnT experiment, Phys. Rev. Lett. **131**, 041003 (2023).

[39] Q. Wang *et al.* (PandaX-II Collaboration), Results of dark matter search using the full PandaX-II exposure, Chin. Phys. C **44**, 125001 (2020).

[40] C. Amole, M. Ardid, I. J. Arnquist, D. M. Asner, D. Baxter, E. Behnke *et al.* (PICO Collaboration), Dark matter search results from the complete exposure of the PICO-60 C_3F_8 bubble chamber, Phys. Rev. D **100**, 022001 (2019).

[41] MAGIC and Fermi-LAT Collaborations, Limits to dark matter annihilation cross-section from a combined analysis of MAGIC and Fermi-LAT observations of dwarf satellite galaxies, J. Cosmol. Astropart. Phys. 02 (2016) 039.

[42] A. Albert *et al.* (Fermi-LAT and DES Collaborations), Searching for dark matter annihilation in recently discovered Milky Way satellites with Fermi-LAT, Astrophys. J. **834**, 110 (2017).
[43] M. Ackermann, A. Albert, B. Anderson, W. B. Atwood, L. Baldini, G. Barbiellini *et al.* (The Fermi-LAT Collaboration), Searching for dark matter annihilation from Milky Way dwarf spheroidal galaxies with six years of Fermi Large Area Telescope data, Phys. Rev. Lett. **115**, 231301 (2015).
[44] H. Baer, K.-Y. Choi, J. E. Kim, and L. Roszkowski, Dark matter production in the early Universe: Beyond the thermal WIMP paradigm, Phys. Rep. **555**, 1 (2015).
[45] P. Huang and C. E. M. Wagner, Blind spots for neutralino dark matter in the MSSM with an intermediate m_A, Phys. Rev. D **90**, 015018 (2014).
[46] D. Das, B. De, and S. Mitra, Cancellation in dark matter-nucleon interactions: The role of non-standard-model-like Yukawa couplings, Phys. Lett. B **815**, 136159 (2021).
[47] M. Drees, M. M. Nojiri, D. P. Roy, and Y. Yamada, Light Higgsino dark matter, Phys. Rev. D **56**, 276 (1997); **64**, 039901(E) (2001).
[48] J. Hisano, S. Matsumoto, M. M. Nojiri, and O. Saito, Direct detection of the Wino and Higgsino-like neutralino dark matters at one-loop level, Phys. Rev. D **71**, 015007 (2005).
[49] J. Hisano, K. Ishiwata, N. Nagata, and T. Takesako, Direct detection of electroweak-interacting dark matter, J. High Energy Phys. 07 (2011) 005.
[50] J. Hisano, K. Ishiwata, and N. Nagata, Direct search of dark matter in high-scale supersymmetry, Phys. Rev. D **87**, 035020 (2013).
[51] N. Baro, F. Boudjema, and A. Semenov, Full one-loop corrections to the relic density in the MSSM: A few examples, Phys. Lett. B **660**, 550 (2008).
[52] N. Baro, F. Boudjema, G. Chalons, and S. Hao, Relic density at one-loop with gauge boson pair production, Phys. Rev. D **81**, 015005 (2010).
[53] A. Chatterjee, M. Drees, and S. Kulkarni, Radiative corrections to the neutralino dark matter relic density—An effective coupling approach, Phys. Rev. D **86**, 105025 (2012).
[54] J. Harz, B. Herrmann, M. Klasen, K. Kovařík, and M. Meinecke, SUSY-QCD corrections to stop annihilation into electroweak final states including Coulomb enhancement effects, Phys. Rev. D **91**, 034012 (2015).
[55] J. Harz, B. Herrmann, M. Klasen, and K. Kovarik, One-loop corrections to neutralino-stop coannihilation revisited, Phys. Rev. D **91**, 034028 (2015).
[56] M. Klasen, K. Kovarik, and P. Steppeler, SUSY-QCD corrections for direct detection of neutralino dark matter and correlations with relic density, Phys. Rev. D **94**, 095002 (2016).
[57] J. Harz, B. Herrmann, M. Klasen, K. Kovařík, and L. P. Wiggering, Precision predictions for dark matter with DM@NLO in the MSSM, arXiv:2312.17206.
[58] S. Bisal, A. Chatterjee, D. Das, and S. A. Pasha, Confronting electroweak MSSM through one-loop renormalized neutralino-Higgs interactions for dark matter direct detection and muon $(g-2)$, arXiv:2311.09938.
[59] N. Aghanim *et al.* (Planck Collaboration), Planck 2015 results. XI. CMB power spectra, likelihoods, and robustness of parameters, Astron. Astrophys. **594**, A11 (2016).
[60] N. Aghanim *et al.* (Planck Collaboration), Planck 2018 results. VI. Cosmological parameters, Astron. Astrophys. **641**, A6 (2020); **652**, C4(E) (2021).
[61] R. Allahverdi, B. Dutta, and K. Sinha, Non-thermal Higgsino dark matter: Cosmological motivations and implications for a 125 GeV Higgs, Phys. Rev. D **86**, 095016 (2012).
[62] L. Aparicio, M. Cicoli, B. Dutta, F. Muia, and F. Quevedo, Light Higgsino dark matter from non-thermal cosmology, J. High Energy Phys. 11 (2016) 038.
[63] M. Tegmark, A. Aguirre, M. Rees, and F. Wilczek, Dimensionless constants, cosmology and other dark matters, Phys. Rev. D **73**, 023505 (2006).
[64] H. Baer, A. Lessa, S. Rajagopalan, and W. Sreethawong, Mixed axion/neutralino cold dark matter in supersymmetric models, J. Cosmol. Astropart. Phys. 06 (2011) 031.
[65] M. Drees, R. Godbole, and P. Roy, Theory and phenomenology of sparticles: An account of four-dimensional $N=1$ supersymmetry in high energy physics (2004).
[66] S. Y. Choi, J. Kalinowski, G. A. Moortgat-Pick, and P. M. Zerwas, Analysis of the neutralino system in supersymmetric theories, Eur. Phys. J. C **22**, 563 (2001); **23**, 769(A) (2002).
[67] G. Bertone, D. Hooper, and J. Silk, Particle dark matter: Evidence, candidates and constraints, Phys. Rep. **405**, 279 (2005).
[68] G. F. Giudice and A. Pomarol, Mass degeneracy of the Higgsinos, Phys. Lett. B **372**, 253 (1996).
[69] V. Barger, M. S. Berger, and P. Ohmann, Supersymmetric particle spectrum, Phys. Rev. D **49**, 4908 (1994).
[70] M. M. El Kheishen, A. A. Shafik, and A. A. Aboshousha, Analytic formulas for the neutralino masses and the neutralino mixing matrix, Phys. Rev. D **45**, 4345 (1992).
[71] G. D. Kribs, A. Martin, and T. S. Roy, Supersymmetry with a chargino NLSP and gravitino LSP, J. High Energy Phys. 01 (2009) 023.
[72] A. Chatterjee, J. Dutta, and S. K. Rai, Natural SUSY at LHC with right-sneutrino LSP, J. High Energy Phys. 06 (2018) 042.
[73] T. Fritzsche and W. Hollik, Complete one loop corrections to the mass spectrum of charginos and neutralinos in the MSSM, Eur. Phys. J. C **24**, 619 (2002).
[74] A. Chatterjee, M. Drees, S. Kulkarni, and Q. Xu, On the on-shell renormalization of the chargino and neutralino masses in the MSSM, Phys. Rev. D **85**, 075013 (2012).
[75] G. Aad *et al.* (ATLAS Collaboration), Searches for electroweak production of supersymmetric particles with compressed mass spectra in $\sqrt{s}=13$ TeV pp collisions with the ATLAS detector, Phys. Rev. D **101**, 052005 (2020).
[76] G. Aad *et al.* (ATLAS Collaboration), Search for long-lived charginos based on a disappearing-track signature using 136 fb^{-1} of pp collisions at $\sqrt{s}=13$ TeV with the ATLAS detector, Eur. Phys. J. C **82**, 606 (2022).
[77] A. Hayrapetyan *et al.* (CMS Collaboration), Search for supersymmetry in final states with disappearing

tracks in proton-proton collisions at $\sqrt{s} = 13$ TeV, arXiv:2309.16823.
[78] G. Aad *et al.* (ATLAS and CMS Collaborations), Combined measurement of the Higgs boson mass in pp collisions at $\sqrt{s} = 7$ and 8 TeV with the ATLAS and CMS experiments, Phys. Rev. Lett. **114**, 191803 (2015).
[79] G. Aad *et al.* (ATLAS Collaboration), Observation of a new particle in the search for the Standard Model Higgs boson with the ATLAS detector at the LHC, Phys. Lett. B **716**, 1 (2012).
[80] S. Chatrchyan *et al.* (CMS Collaboration), Observation of a new boson at a mass of 125 GeV with the CMS experiment at the LHC, Phys. Lett. B **716**, 30 (2012).
[81] M. Carena, S. Heinemeyer, O. Stål, C. E. M. Wagner, and G. Weiglein, MSSM Higgs boson searches at the LHC: Benchmark scenarios after the discovery of a Higgs-like particle, Eur. Phys. J. C **73**, 2552 (2013).
[82] G. Alguero, J. Heisig, C. Khosa, S. Kraml, S. Kulkarni, A. Lessa *et al.*, Constraining new physics with SModelS version 2, arXiv:2112.00769.
[83] J. Heisig, S. Kraml, and A. Lessa, Constraining new physics with searches for long-lived particles: Implementation into SModelS, arXiv:1808.05229.
[84] J. Dutta, S. Kraml, A. Lessa, and W. Waltenberger, SModelS extension with the CMS supersymmetry search results from Run 2, Lett. High Energy Phys. **1**, 5 (2018).
[85] F. Ambrogi, S. Kraml, S. Kulkarni, U. Laa, A. Lessa, V. Magerl *et al.*, SModelS v1.1 user manual, arXiv:1701.06586.
[86] F. Ambrogi *et al.*, SModelS v1.2: Long-lived particles, combination of signal regions, and other novelties, arXiv:1811.10624.
[87] T. Sjöstrand, S. Ask, J. R. Christiansen, R. Corke, N. Desai, P. Ilten *et al.*, An introduction to PYTHIA 8.2, Comput. Phys. Commun. **191**, 159 (2015).
[88] T. Sjostrand, S. Mrenna, and P. Z. Skands, PYTHIA 6.4 physics and manual, J. High Energy Phys. 05 (2006) 026.
[89] W. Beenakker, R. Hopker, M. Spira, and P. Zerwas, Squark and gluino production at hadron colliders, Nucl. Phys. **B492**, 51 (1997).
[90] A. Buckley, PySLHA: A pythonic interface to SUSY Les Houches Accord data, arXiv:1305.4194.
[91] G. Belanger, F. Boudjema, A. Pukhov, and A. Semenov, Dark matter direct detection rate in a generic model with micrOMEGAs 2.2, Comput. Phys. Commun. **180**, 747 (2009).
[92] M. Drees and M. M. Nojiri, Neutralino-nucleon scattering reexamined, Phys. Rev. D **48**, 3483 (1993).
[93] M. Drees and M. M. Nojiri, New contributions to coherent neutralino-nucleus scattering, Phys. Rev. D **47**, 4226 (1993).
[94] J. Ellis and R. A. Flores, Elastic supersymmetric relic-nucleus scattering revisited, Phys. Lett. B **263**, 259 (1991).
[95] J. Ellis and R. A. Flores, Prospects for neutralino detection with a ^{73}Ge $+^{76}$ Ge detector, Phys. Lett. B **300**, 175 (1993).
[96] M. Shifman, A. Vainshtein, and V. Zakharov, Remarks on Higgs-boson interactions with nucleons, Phys. Lett. **78B**, 443 (1978).
[97] G. Belanger, F. Boudjema, A. Pukhov, and A. Semenov, micrOMEGAs_3: A program for calculating dark matter observables, Comput. Phys. Commun. **185**, 960 (2014).
[98] P. D. Group, R. L. Workman, V. D. Burkert, V. Crede, E. Klempt, U. Thoma *et al.*, Review of particle physics, Prog. Theor. Exp. Phys. **2022**, 083C01 (2022).
[99] J. R. Ellis, K. A. Olive, and C. Savage, Hadronic uncertainties in the elastic scattering of supersymmetric dark matter, Phys. Rev. D **77**, 065026 (2008).
[100] A. Djouadi and M. Drees, QCD corrections to neutralino nucleon scattering, Phys. Lett. B **484**, 183 (2000).
[101] G. Belanger, F. Boudjema, A. Pukhov, and A. Semenov, micrOMEGAs: Version 1.3, Comput. Phys. Commun. **174**, 577 (2006).
[102] G. Alguero, G. Belanger, S. Kraml, and A. Pukhov, Co-scattering in micrOMEGAs: A case study for the singlet-triplet dark matter model, SciPost Phys. **13**, 124 (2022).
[103] W. Porod, SPheno, A program for calculating supersymmetric spectra, SUSY particle decays and SUSY particle production at e^+e^- colliders, Comput. Phys. Commun. **153**, 275 (2003).
[104] J. Küblbeck, M. Böhm, and A. Denner, FeynArts—Computer-algebraic generation of Feynman graphs and amplitudes, Comput. Phys. Commun. **60**, 165 (1990).
[105] T. Hahn, Generating Feynman diagrams and amplitudes with FeynArts 3, Comput. Phys. Commun. **140**, 418 (2001).
[106] T. Hahn and M. Pérez-Victoria, Automated one-loop calculations in four and d dimensions, Comput. Phys. Commun. **118**, 153 (1999).
[107] T. Fritzsche, T. Hahn, S. Heinemeyer, F. von der Pahlen, H. Rzehak, and C. Schappacher, The implementation of the renormalized complex MSSM in FeynArts and FormCalc, Comput. Phys. Commun. **185**, 1529 (2014).
[108] G. Belanger, F. Boudjema, A. Pukhov, and A. Semenov, micrOMEGAs 2.0: A program to calculate the relic density of dark matter in a generic model, Comput. Phys. Commun. **176**, 367 (2007).
[109] G. Belanger, F. Boudjema, A. Pukhov, and A. Semenov, micrOMEGAs: A tool for dark matter studies, Nuovo Cimento Soc. Ital. Fis. **033N2C**, 111 (2010).
[110] F. Staub, SARAH 4: A tool for (not only SUSY) model builders, Comput. Phys. Commun. **185**, 1773 (2014).
[111] N. Baro and F. Boudjema, Automatized full one-loop renormalization of the MSSM. II. The chargino-neutralino sector, the sfermion sector, and some applications, Phys. Rev. D **80**, 076010 (2009).
[112] G. Passarino and M. Veltman, One-loop corrections for e^+e^- annihilation into $\mu^+\mu^-$ in the Weinberg model, Nucl. Phys. **B160**, 151 (1979).
[113] H. H. Patel, Package-X: A *Mathematica* package for the analytic calculation of one-loop integrals, Comput. Phys. Commun. **197**, 276 (2015).
[114] G. van Oldenborgh, FF—A package to evaluate one-loop Feynman diagrams, Comput. Phys. Commun. **66**, 1 (1991).
[115] M. Frank, T. Hahn, S. Heinemeyer, W. Hollik, H. Rzehak, and G. Weiglein, The Higgs boson masses and mixings of the complex MSSM in the Feynman-diagrammatic approach, J. High Energy Phys. 02 (2007) 047.